MCR-70-296

CR 115280

N72-13583 (NASA-CR-115280) CMG ASSEMBLY LIFE TEST AND ENGINEERING EVALUATION TEST, M-509 EXPERIMENT P.S. Craner, et al (Martin Marietta Corp.) Jun. 1970 35 p CSCL 17G
Unclas G3/21 10884
(NASA CR OR TMX OR AD NUMBER) (CATEGORY)
FACILITY

NATIONAL AER

OFFICE OF PRIME RESPONSIBILITY

KW

DEC 1971
RECEIVED

ASTRONAUT MANEUVERING EQUIPMENT

NAS9-9339

CMG ASSEMBLY LIFE TEST AND ENGINEERING EVALUATION TEST

DENVER DIVISION

OPEN

CMG ASSEMBLY LIFE TEST
AND ENGINEERING EVALUATION TEST
M-509 EXPERIMENT

CONTRACT NAS9-9339

JUNE 1970

MCR-70-296

PREPARED BY: P. S. Cramer
J. T. Josephson

APPROVED BY: J. R. Tewell
Technical Director
M-509

FOREWORD

This report has been prepared by Martin Marietta and is submitted in accordance with Contract NAS9-9339 paragraph 8.1.8 of Exhibit 'B', MSC-KW-E-69-13, the Flight Hardware End Item Specification.

ABSTRACT

The first M-509 CMG Assembly produced by Sperry was a design development test article. The CMGA underwent EMI, functional, and environmental testing by Sperry during March, April, and May, 1970. The unit was shipped to MMC where it was tested from May 16 to June 15 prior to installation into the ASMU Engineering Development Model. These tests consisted of a life test and engineering evaluation tests that included a one axis air bearing table. The tests and results are described in this report.

TABLE OF CONTENTS

	TITLE	PAGE
I.	INTRODUCTION	1
II.	INITIAL SETUP AND CHECKOUT	1
III.	LIFE TEST	2
IV.	ENGINEERING EVALUATION TESTS	7
	Command Rate and Torquer Current Transfer	7
	Cage and Lock	7
	Static Inverter and Signal Noise Tests	7
	Dynamic Response Tests	14
	Closed Loop Drift Rate Tests	14
	Gimbal Disturbance Torque Evaluation Tests	14

LIST OF FIGURES

	FIGURE	PAGE
1	SYSTEM RESPONSE TO 7 VDC TORQUER INPUT	4
2	SYSTEM RESPONSE TO 14 VDC CHANGE IN TORQUER INPUT	5
3	SYSTEM RESPONSE FOR 1 TORQUING CYCLE	6
4	TORQUING CURRENT AND COMMAND TRANSFER ROLL AXIS	8
5	TORQUING CURRENT AND COMMAND TRANSFER PITCH AXIS	9
6	TORQUING CURRENT AND COMMAND TRANSFER YAW AXIS	10
7	TORQUING CURRENT AND OUTPUT RATE vs GIMBAL ANGLE FOR CONSTANT 3 VDC COMMAND ROLL AXIS	11
8	CURRENT vs VOLTAGE AT NO LOAD	12
9	CURRENT vs VOLTAGE AT RATED LOAD	13
10	ROLL DRIFT RATE vs GIMBAL ANGLE	15
11	PITCH DRIFT RATE vs GIMBAL ANGLE	16
12	YAW DRIFT RATE vs GIMBAL ANGLE	17
13	CMG ONE AXIS TORQUE DIAGRAM	18
14	CMG COORDINATE SYSTEM	21
15	X GYRO FRICTION TORQUE	25
16	Y GYRO FRICTION TORQUE	26
17	Z GYRO FRICTION TORQUE	27
18	X GYRO REACTION TORQUE	28
19	Y GYRO REACTION TORQUE	29
20	Z GYRO REACT[illegible]	[illegible]

LIST OF TABLES

	TITLE	PAGE
1	POSITION MATRIX FOR DRIFT COMPONENTS	20
2	MASS UNBALANCE TORQUES	24

I. INTRODUCTION

Martin Company received the design development Control Moment Gyro system from Sperry on 16 May, 1970. This unit is intended to be installed in the Engineering Development Model ASMU for evaluation tests of the system hardware. Prior to installation of the CMG into the EDM system test program, certain tests were required of the CMG unit to assure interface compatibility, functional performance capability, and design integrity for mission life. The purpose of this report is to describe the procedures and document the results of the life test and the engineering evaluation tests that were performed to accomplish these objectives.

When the CMG unit was delivered to Martin on 16 May, 1970, it had a total elapsed test running time of 91.7 hours. Life tests at MMC required 75.0 hours and engineering evaluation tests at MMC required 52.3 hours. Total system run time on the CMG unitwas 218.0 hours at the completion of the tests on 15 June.

II. INITIAL SETUP AND CHECKOUT

Hardware setup in the test holding fixture and interface wiring checkout was completed on May 16. Interface wiring at J101 of the CMG was checked to be compatible with the wire list of PD9600014.

Power was applied to the unit and preliminary checkout of the input output signals on a qualitative basis was complete on May 18. During this time three important discrepancies with the procurement drawing were noted. These are listed below with the appropriate action taken to alleviate the problem.

1. Reversed input/output torquing transfer polarity on all axes. This discrepancy if undetected would have resulted in reversed transfer between the rotational controller commands and the resulting output rate, and incorrect thruster commands wherever desaturation or coarse cage was required. On May 28, the problem was fixed by Sperry at Denver. This was accomplished by reversing the spin rotation direction on all six wheels.

2. Wheel speed pickoff outputs produced negative voltages at speeds less than 16,000 rpm. When the wheels were not rotating this voltage ranged from -2.0 to -7.0 VDC depending on time from power application and specific output. This discrepancy if undetected would have resulted in negative input voltages to the telemetry subsystem that would exceed the design limits. On June 4, the problem was corrected by Sperry at Denver. This was accomplished by placing a diode at the output on each amplifier. Layout was previously designed on the printed circuit boards to facilitate the diodes since the original Sperry design included this feature.

3. Noise on the static inverter power outputs exceeds the specified 50 mv peak to peak requirements. This noise appears as spikes spaced evenly at 0.16 milliseconds (6.4 kc). The spikes have a duration of approximately 0.2 microseconds and an amplitude between 20 and 150 millivolts depending on load and other factors. It is not presently known what effect, if any, the noise will have on total system performance when the CMG's are mounted in the EDM hardware for functional test.

All signals were investigated during the initial setup and checkout of the CMG unit. This investigation included picture taking of scope traces on all output signals. Documentation of these findings is included in the engineering evaluation section of this report.

III. LIFE TEST

Conditions for the life test were specified on 19 May at Denver. These conditions resulted from exercising the CMG unit on a floated single axis gas bearing during initial setup and checkout. With a total floated moment of inertia of 18 slug-ft^2, the peak gimbal rate of 7 radians per second is produced with a +7 or -7 volt step command to the torquer drive electronics. A +7 to -7 volt step command produces a 13 radian per second peak gimbal rate. Response to these inputs is shown in Figures 1 and 2. Gimbal impact on the stops is indicated by the abrupt change in gimbal rate. After impact the gimbal oscillates against the spring until damping removes the energy in the gimbal gained during the swing. In order to attain the 14 radian per second gimbal rate with a 14 volt change in torquer command it is necessary to provide the proper initial table rate and gimbal angle. This is shown in Figure 2.

The life test was initiated on 19 May, 1970, according to the following sequence:

a. The CMGA was mounted on the air bearing table with the roll output axis parallel to the table axis.

b. The spin motors were energized and run up for 20 minutes.

c. Step input commands were issued to the roll axis every 20 seconds to cause a pair of gimbal rate spikes (one positive and one negative) of 6 to 8 radians/second and every 200 seconds to cause a pair of gimbal rate spikes (one positive and one negative) of 12 to 15 radians/second. A total of 260 small spikes and 26 large spikes were accumulated over a period of about 45 minutes. Typical response to these inputs is shown in Figure 3.

d. The CMGA was run without command for a period of 60 minutes.

e. The spin motors were allowed to run down for 30 minutes.

f. Steps b through e were repeated for a total of 10 cycles for a total accumulation of 2600 small spikes and 260 large spikes.

g. The pitch axis was aligned with the table axis and steps b through f repeated for the pitch axis.

h. The yaw axis was aligned with the table axis and steps b through f repeated for the yaw axis.

Torquing commands, gimbal angle rate, table rate, wheel speeds, and system current, were recorded for the duration of the life test. This data has been retained on strip charts and is available for display. A small portion of the strip chart data was used for Figures 1, 2, and 3.

During the 75 hour life test there was no major degradation of system performance. Subsequent drift rates and gimbal disturbance torque evaluation tests conducted after the life test disclosed only small increases in bearing friction and negligible reaction torque shifts. These tests have proved to be quite accurate in determining CMG quality and will be performed before and after any similar tests conducted on the CMGs in the future.

The life test proceeded from 19 May through 27 May on a split shift basis for 15 hours each day. No interruptions were encountered due to the CMG unit, and the test proceeded smoothly to its conclusion.

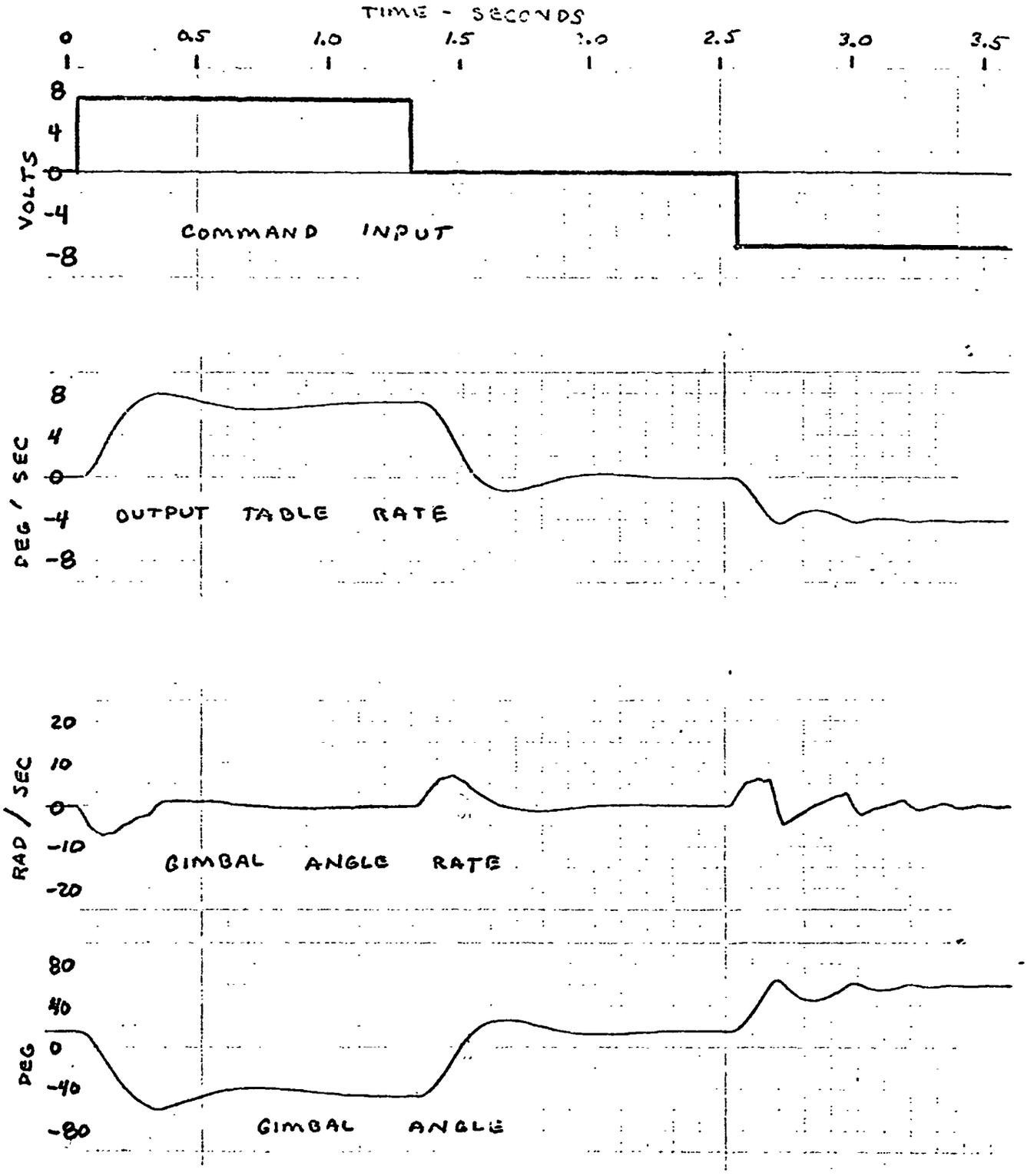

FIGURE 1

SYSTEM RESPONSE TO 7 VDC TORQUER INPUT

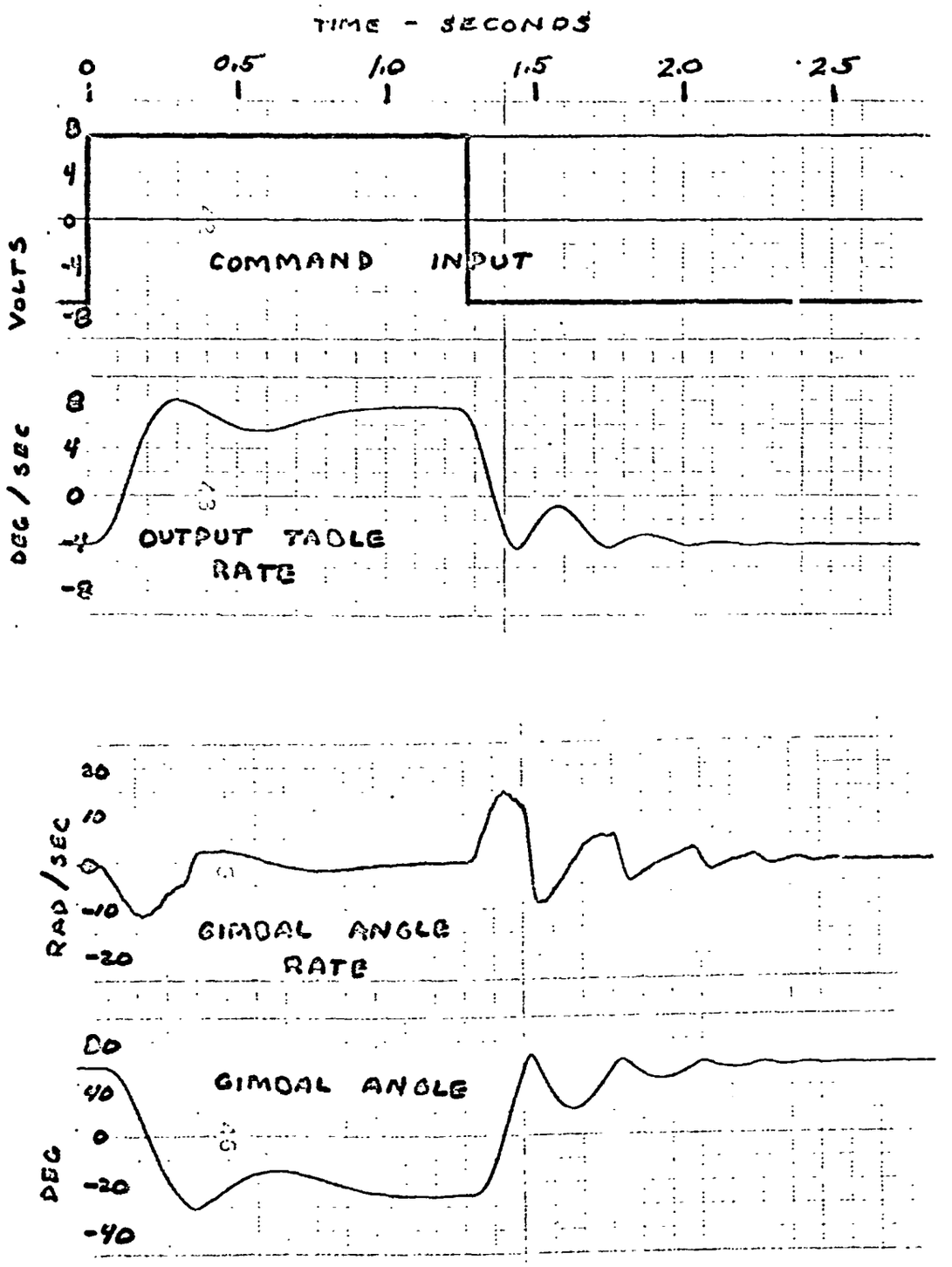

FIGURE 2.

SYSTEM RESPONSE TO 14 VDC CHANGE

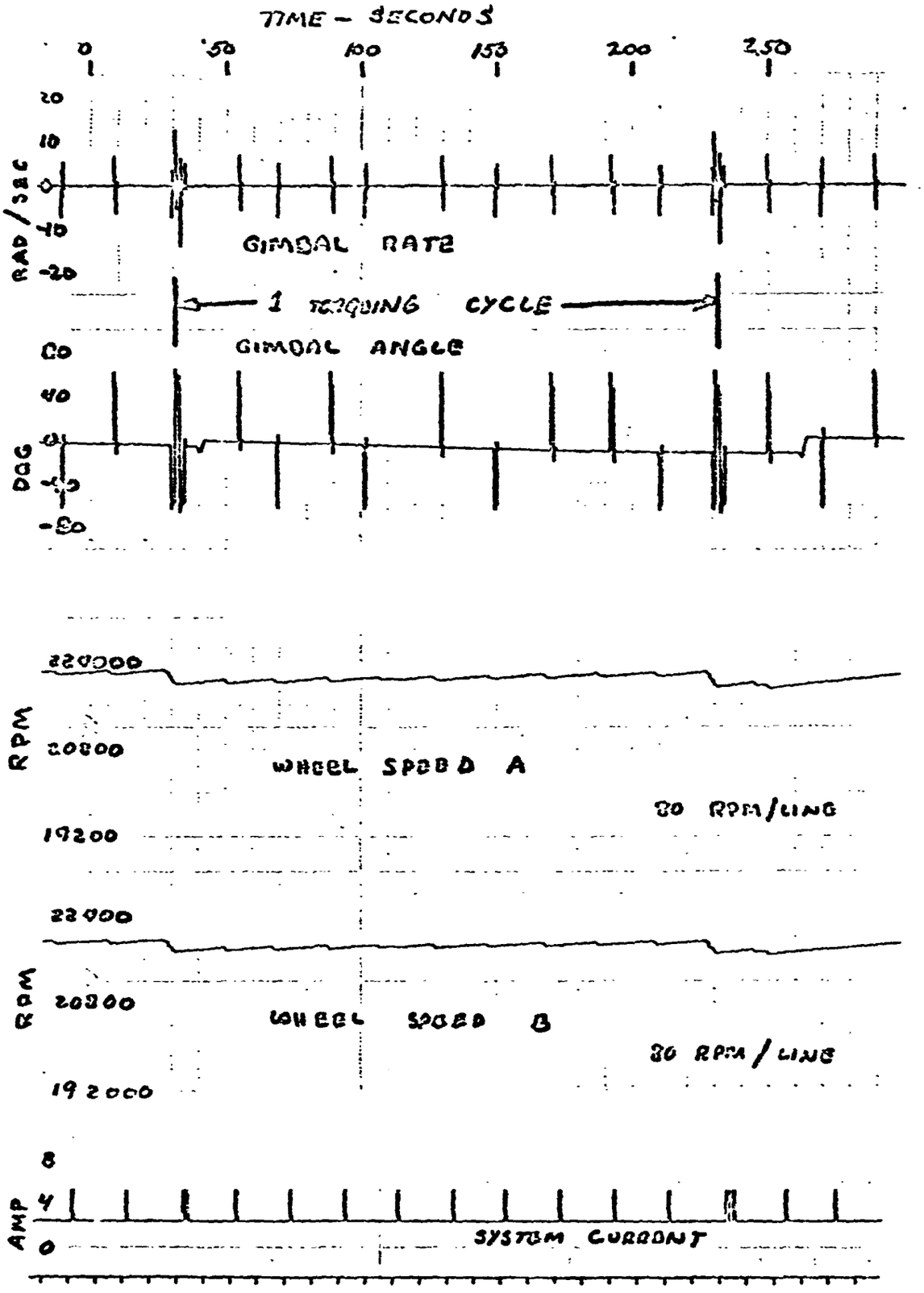

FIGURE 3

SYSTEM RESPONSE FOR 1 TORQUING CYCLE

IV. ENGINEERING EVALUATION TESTS

Engineering evaluation tests began on 28 May. The desired objective of these tests is to assure the functional performance of the CMG unit on a system basis. To this extent, possible problems could be dispersed with before the unit was installed in the EDM hardware.

Command Rate and Torquer Current Transfer - The test was accomplished by placing a known command input voltage to the torquer drive electronics and measuring the resulting current and floated table rate for steady state conditions. Results of the measurements are shown in Figures 4, 5, and 6 for the roll, pitch and yaw axes, respectively. The resulting rate command transfer is within the expected limits and is linear to commands of ± 5 volts. The resulting torquer current - rate output transfer has a greater torque/current gain than originally anticipated. This will result in some savings in required torquer power. Furthermore, this transfer is not linear as expected. Torquer conformity is shown in Figure 7 for one roll axis.

Cage and Lock - A breadboard Control Electronics Assembly was interfaced with the signals from the Control Moment Gyro Assembly. The CEA produced the appropriate commands to a set of thrusters mounted on the airbearing table. For this setup, the interaction between the thruster system and CMG Assembly were demonstrated to operate correctly for desaturation and cage and lock functions. Gimbal angle to torquer gain during fine cage is somewhat less than expected. With a lock window of ± 0.25 degrees, a constant body rate of 0.1 degrees per second will produce gimbal torques sufficient to standoff the gimbal angle beyond the window and lock will not occur. Subsequent units will be built with a ± 0.7 deg lock window.

Static Inverter and Signal Noise Tests - Tests on the static inverter were performed at no load and rated load of the power supply outputs. Results of these tests are provided in Figures 8 and 9. At rated load and rated voltage (28.0 VDC) the CMG unit requires 4.67 amp to power the six wheels at steady state speed, torquer drive electronics, and static inverter. This 4.67 amp is exclusive of the command torquer current.

Photographs of all CMG output signals were taken on the scope traces. Noise spikes exist on all outputs. Most significant of this noise is the spikes on the six analog wheel speed outputs. This noise consists of a triangle wave at 1.1 KC at 0.05 volts peak to peak. At the peaks of this triangle wave are spikes of 1.0 to 2.0 volts for a duration of 12 microseconds.

Noise spikes of 15 microseconds duration, and 100 to 300 millivolts peak to peak amplitude at 6.4 KC exists on the gimbal angle outputs and the TM gimbal angle outputs.

10 X 10 TO THE CENTIMETER 46 1517
KEUFFEL & ESSER CO.

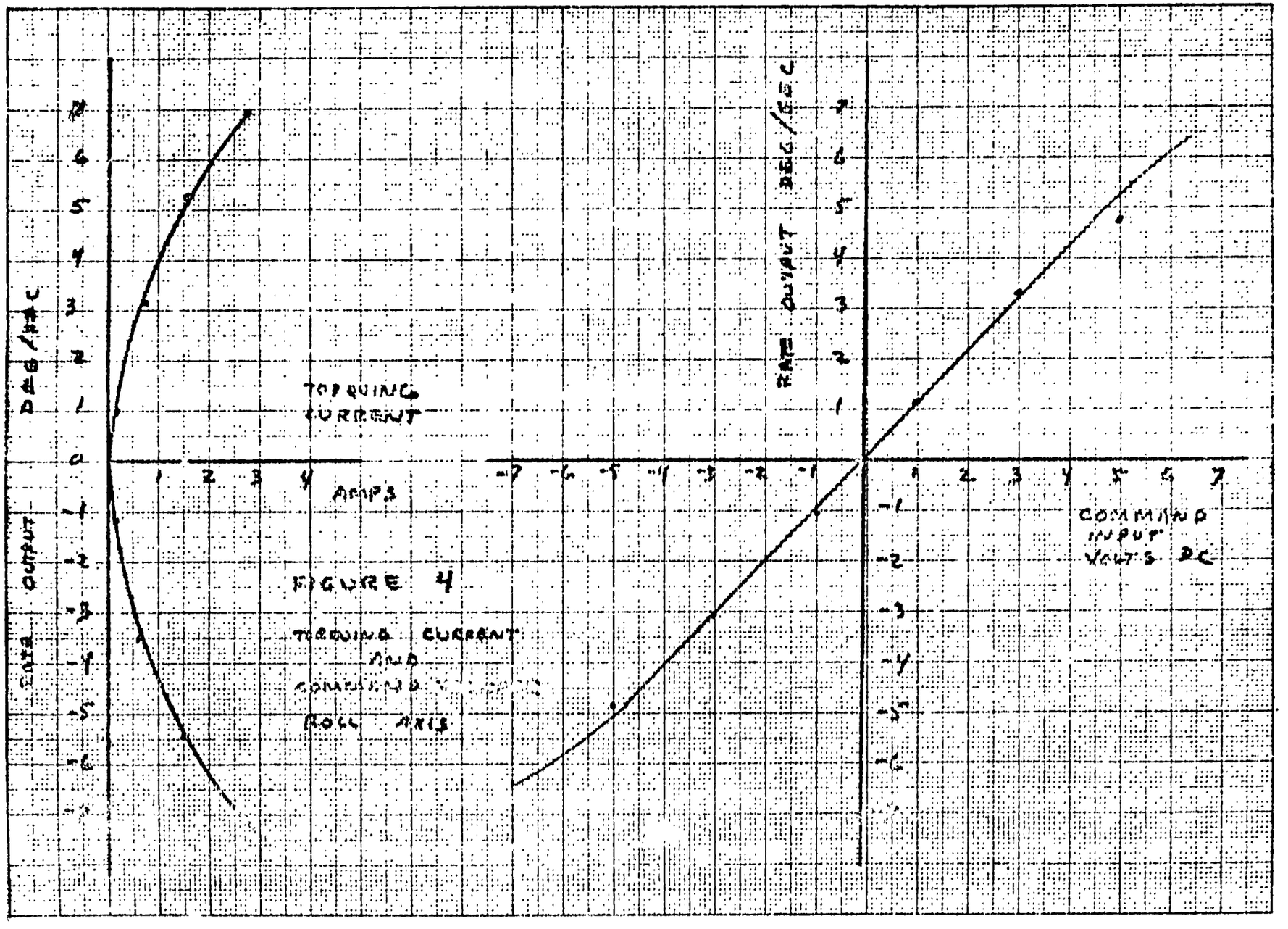

FIGURE 4

TORQUING CURRENT AND COMMANDED [illegible] ROLL AXIS

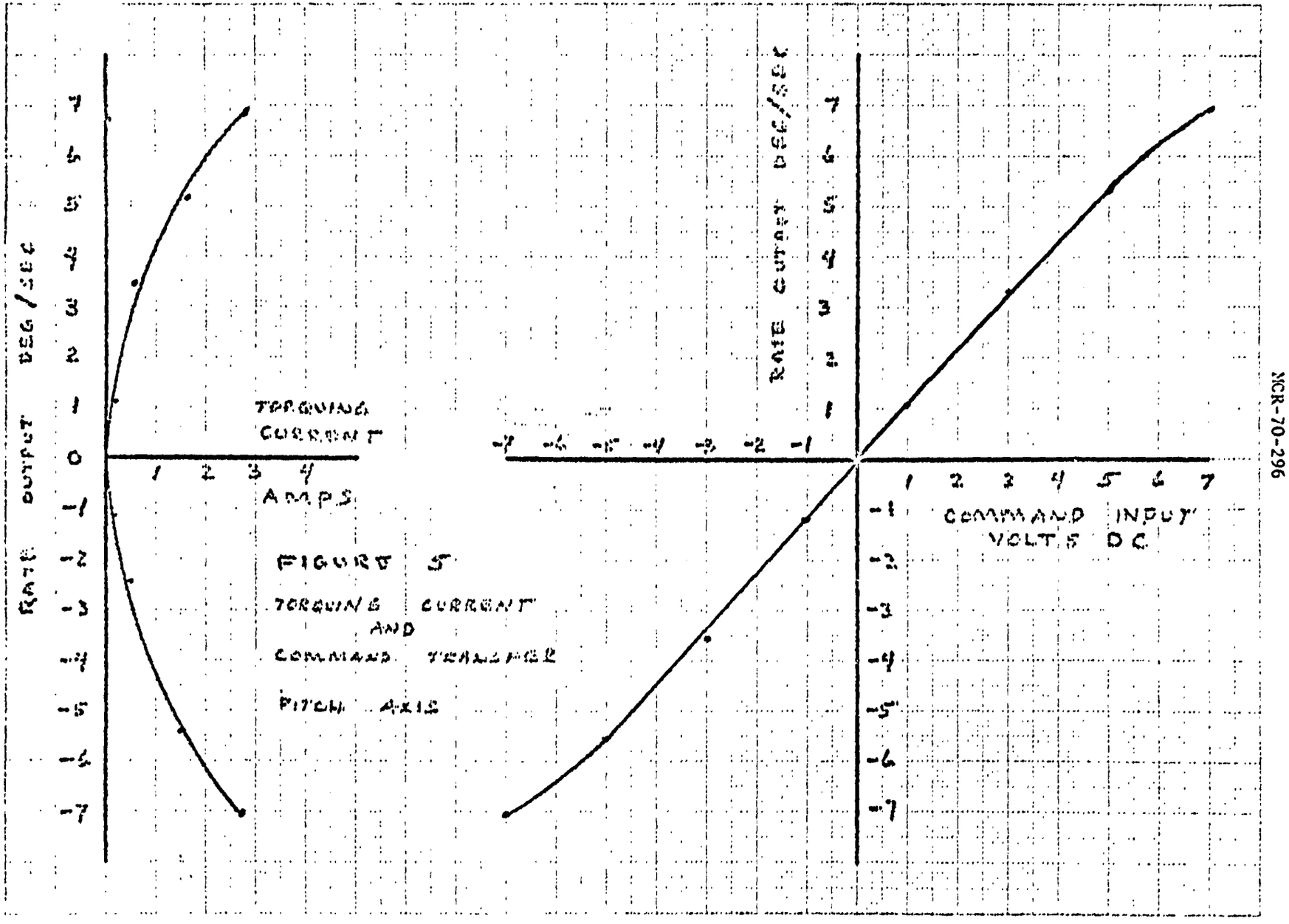

FIGURE 5
TORQUING CURRENT AND COMMAND TRANSFER
PITCH AXIS

REPRODUCIBILITY OF THE ORIGINAL PAGE IS POOR

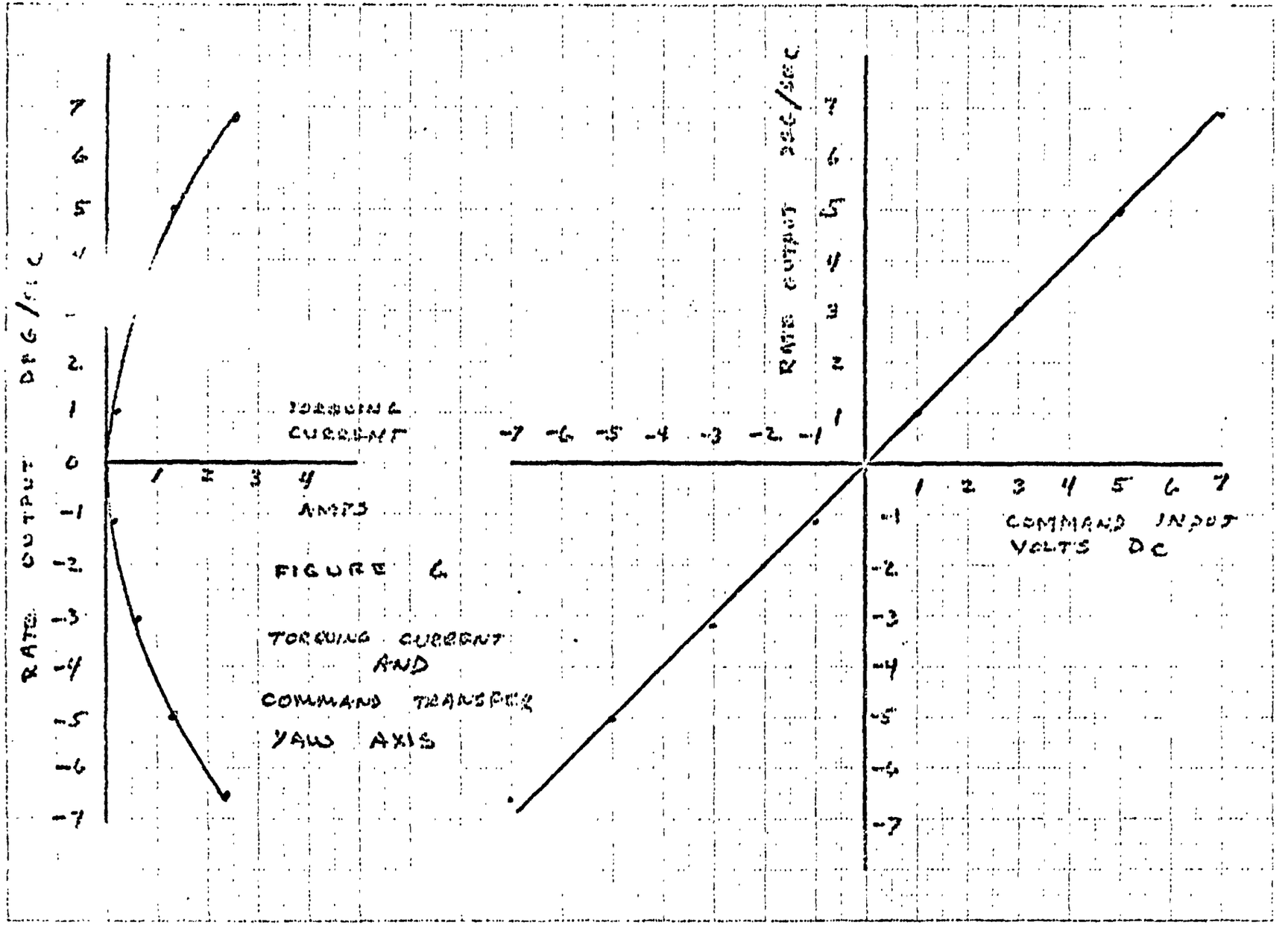

FIGURE 6

TORQUING CURRENT AND COMMAND TRANSFER YAW AXIS

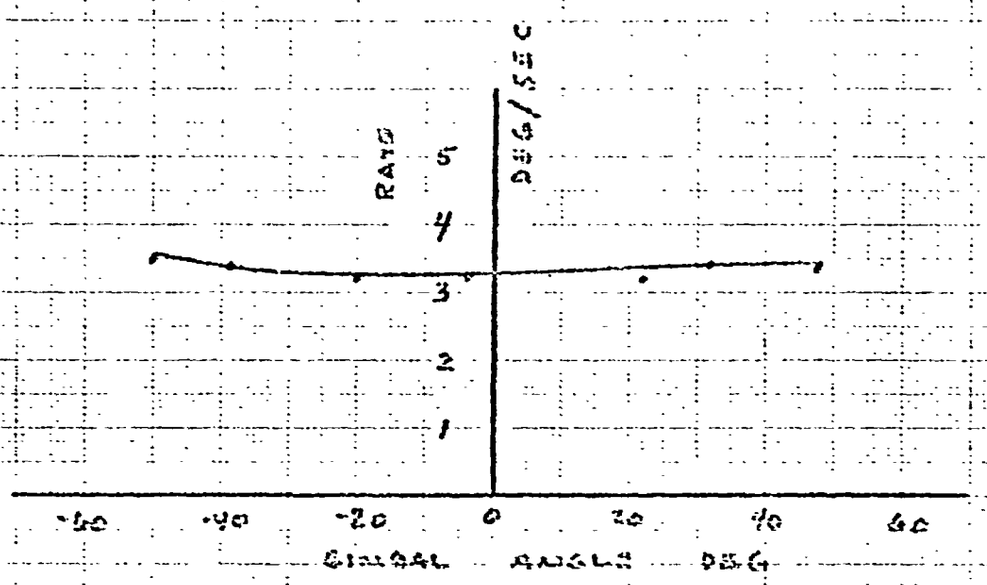

FIGURE 7

TORQUING CURRENT AND OUTPUT RATES VS GIMBAL ANGLE FOR CONSTANT 3 VDC COMMAND ROLL AXIS

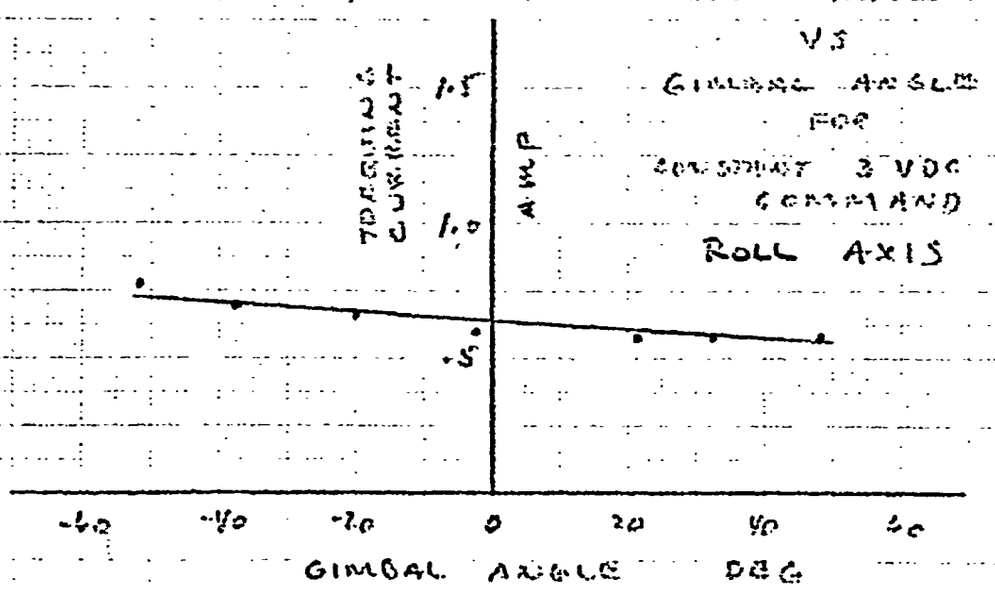

FIGURE 8

CURRENT VS VOLTAGE AT NO LOAD

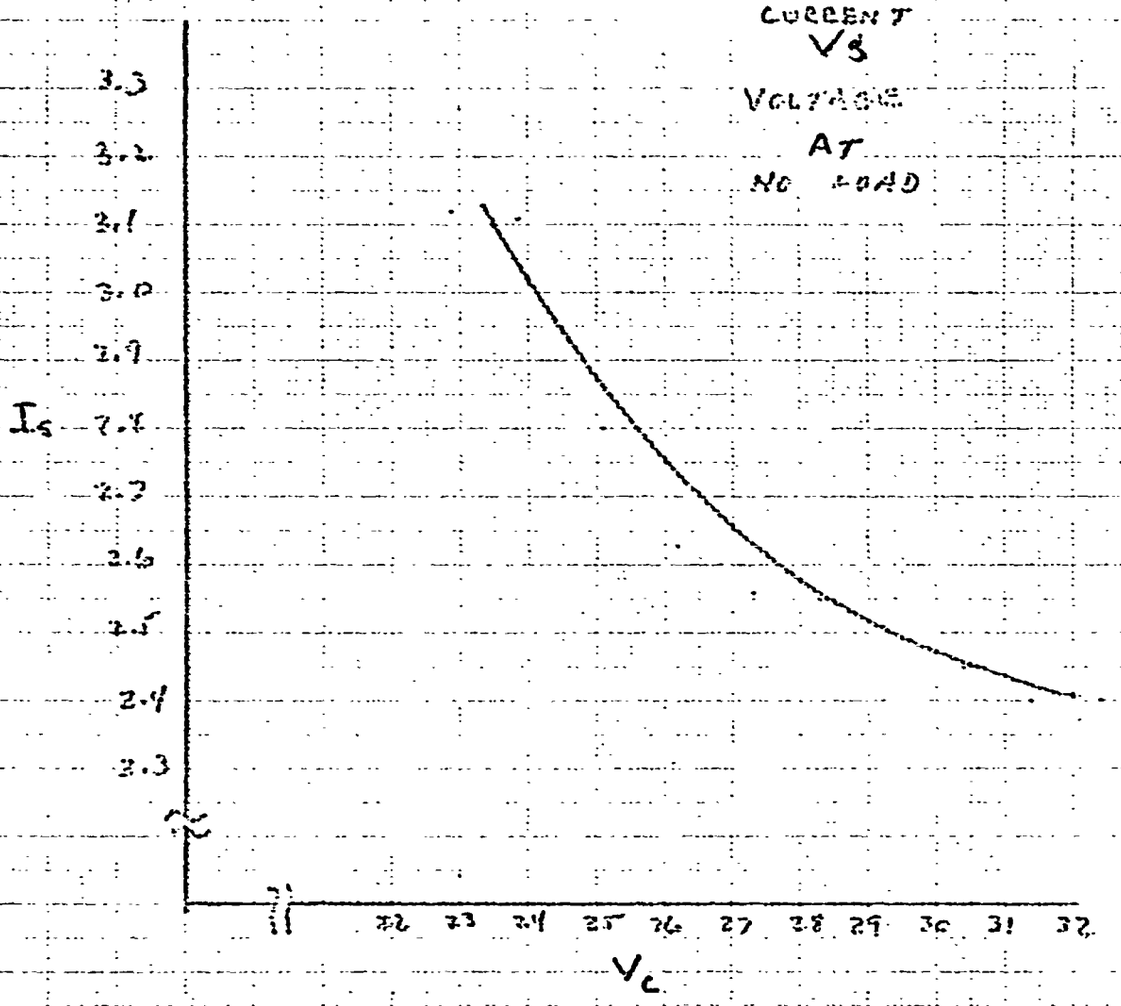

V_s	I_s	V_c
25.0	3.12	22.9
26.0	3.10	23.9
27.0	2.80	25.1
28.0	2.65	26.2
29.0	2.56	27.3
30.0	2.55	28.3
31.0	2.50	29.3
32.0	2.45	30.4
33.0	2.40	31.4
34.0	2.40	32.4

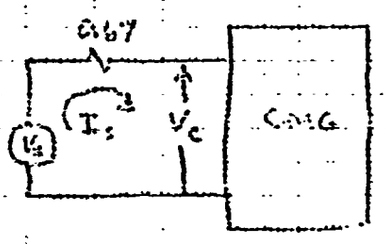

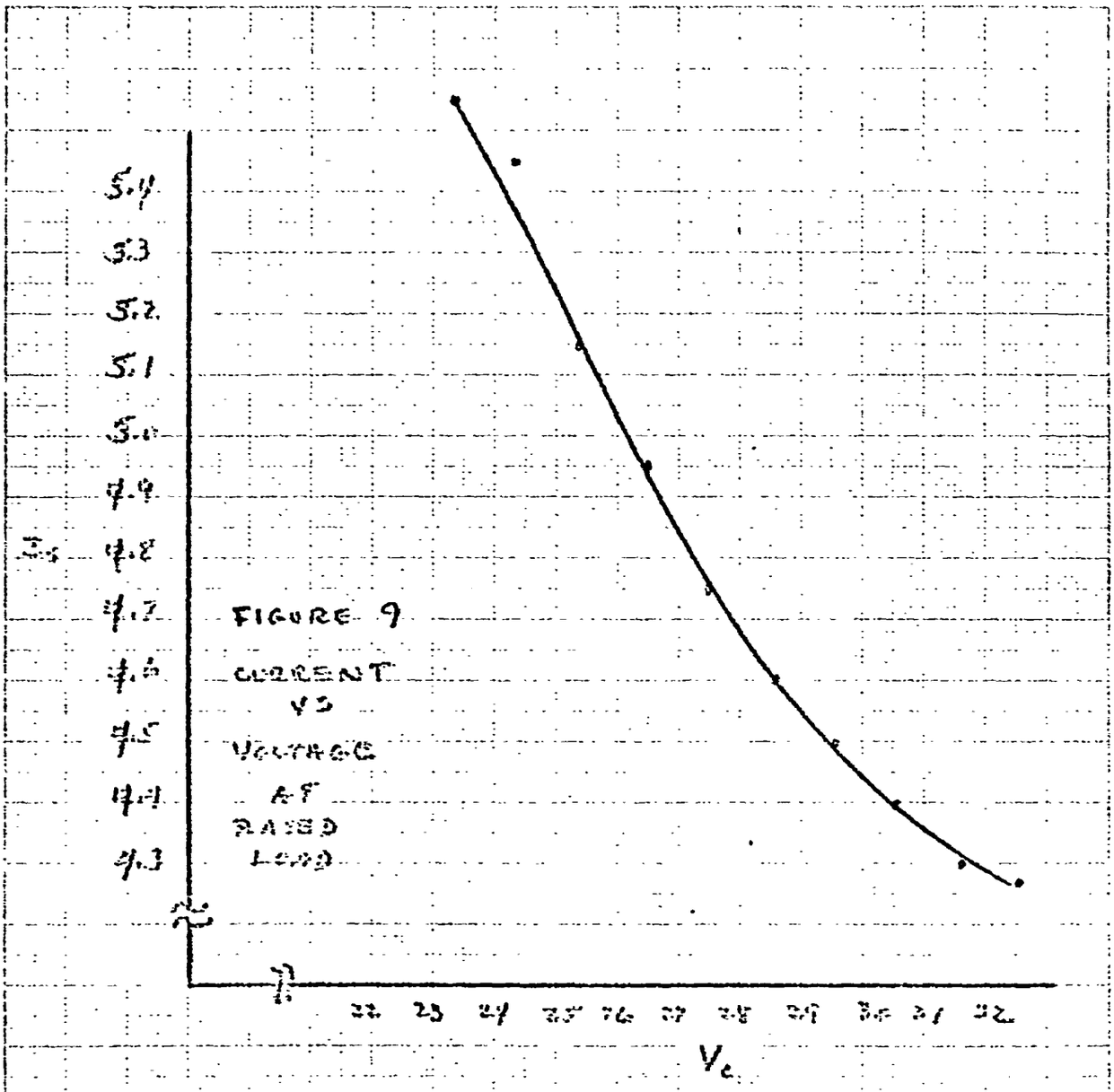

FIGURE 9

CURRENT VS VOLTAGE AT RATED LOAD

V_s	I_s	V_c
25.0	5.55A	23.3
26.0	5.45A	24.3
27.0	5.15	25.4
28.0	4.95	26.5
29.0	4.75	27.5
30.0	4.60	28.6
31.0	4.50	29.6
32.0	4.40	30.6
33.0	4.30	31.7
34.0	4.275	32.7

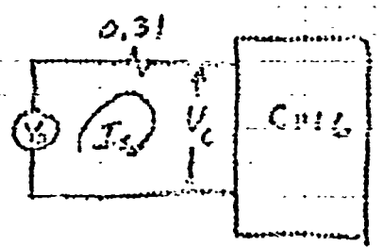

Dynamic Response Tests - The dynamic response while mounted to a rigid floating fixture was measured with a total inertia of 13.5, 15.5, and 6.4 slug ft^2 about the roll, pitch, and yaw axes respectively with step command inputs from 1 to 5 volts. The response approximated a second order system with rise time to 90% of steady state of 0.12 to 0.20 seconds for roll, 0.12 to 0.14 seconds for pitch, and 0.07 seconds for yaw.

Closed Loop Drift Rate Tests - System closed loop drift rate was measured with the use of the air bearing and a calibrated rate gyro. This was accomplished by unlocking the CMG pair with the output axis parallel to the table rotation axis, compensating for wire torques existing between the room and the table top, and measuring the table rate at various gimbal angles. The resulting drift rate is due to gimbal mass unbalance, earth rate, gimbal reaction torque and gimbal stiction-friction torque. Data from these tests is displayed in Figures 10, 11, and 12 for the roll, pitch, and yaw axes respectively. Note that on these plots the data is plotted as points. The lines are predicted drift rates based on data from measuring the gimbal disturbance torques as explained in the next section of this report.

Gimbal Disturbance Torque Evaluation Tests - Certain undesirable torques are present about the CMG gimbals that tend to degrade the attitude hold mode. These gimbal disturbance torques will cause the AMRV to drift rotationally relative to the inertial coordinate frame. The primary disturbance torques in the CMG are static friction torque, magnetic reaction torque, flex lead reaction torque, spin axis mass unbalance, and output axis mass unbalance.

Figure 13 is a one axis block diagram of the CMG showing how the torques are summed at the CMG gimbals. The symbols are defined as follows:

δ	Input command voltage
K_m	Forward loop gain including torquer amplifier and torque motor, 7.04 oz. in/volt
K_d	Damping feedback gain
T_f	Static friction torque
T_r	Reaction torque, including magnetic and flex lead torque
T_o	Output axis mass unbalance torque
T_s	Spin axis mass unbalance torque
T_{IA}	Sum of torques about the input axis
T_{OA}	Torque applied to the output axis

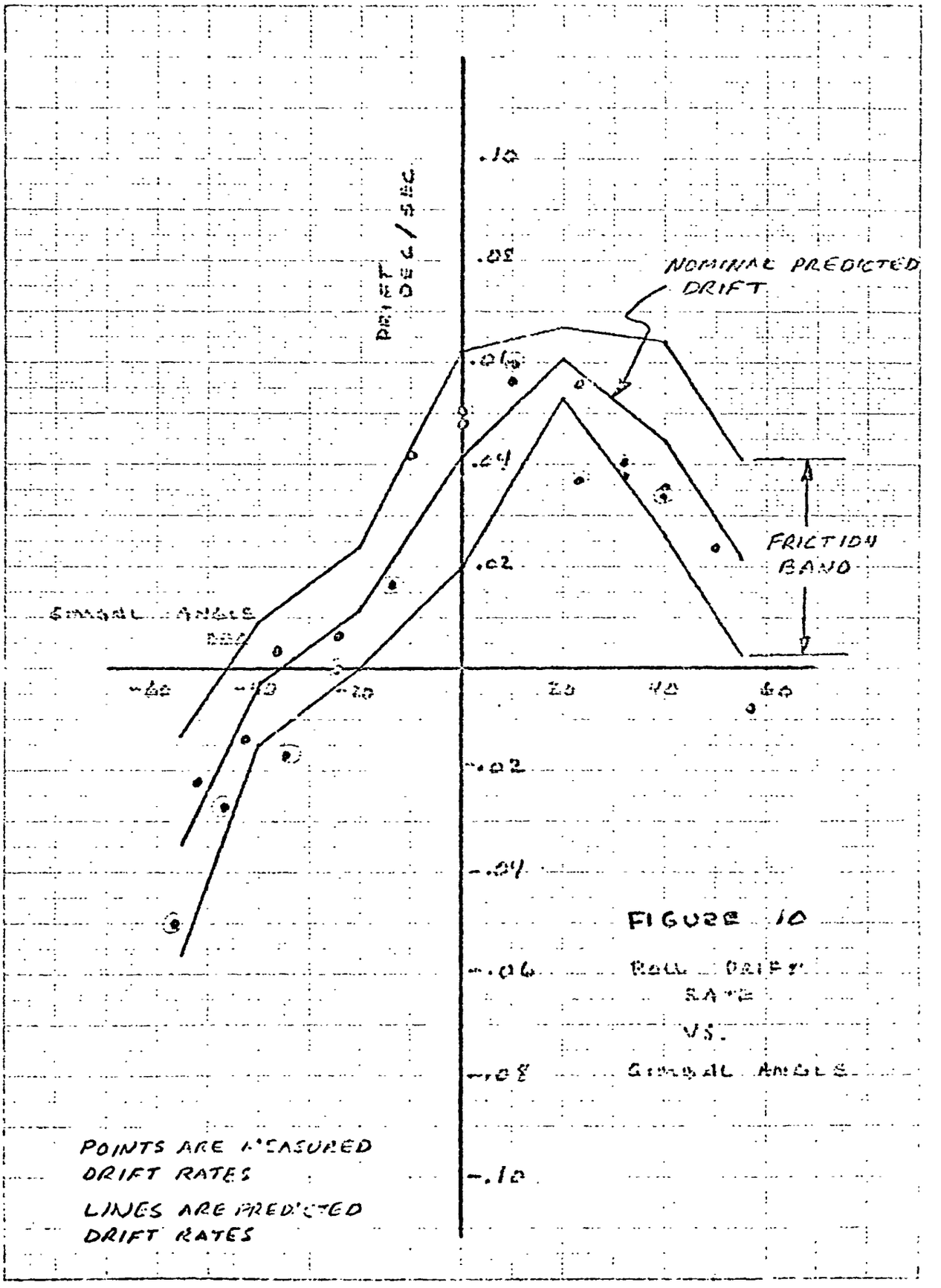

FIGURE 10

ROLL DRIFT RATE VS. GIMBAL ANGLE

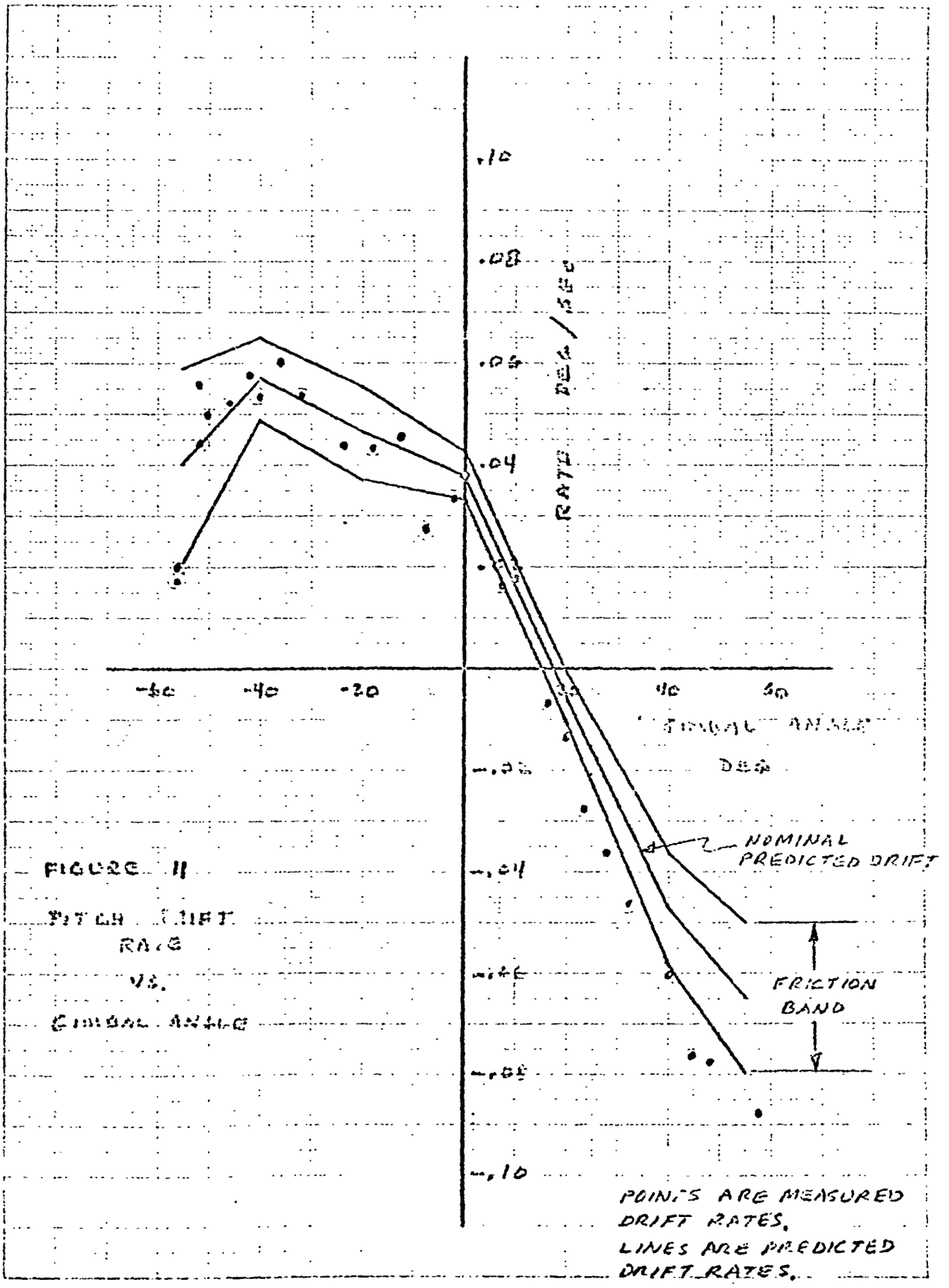

FIGURE 11

PITCH DRIFT RATE VS. GIMBAL ANGLE

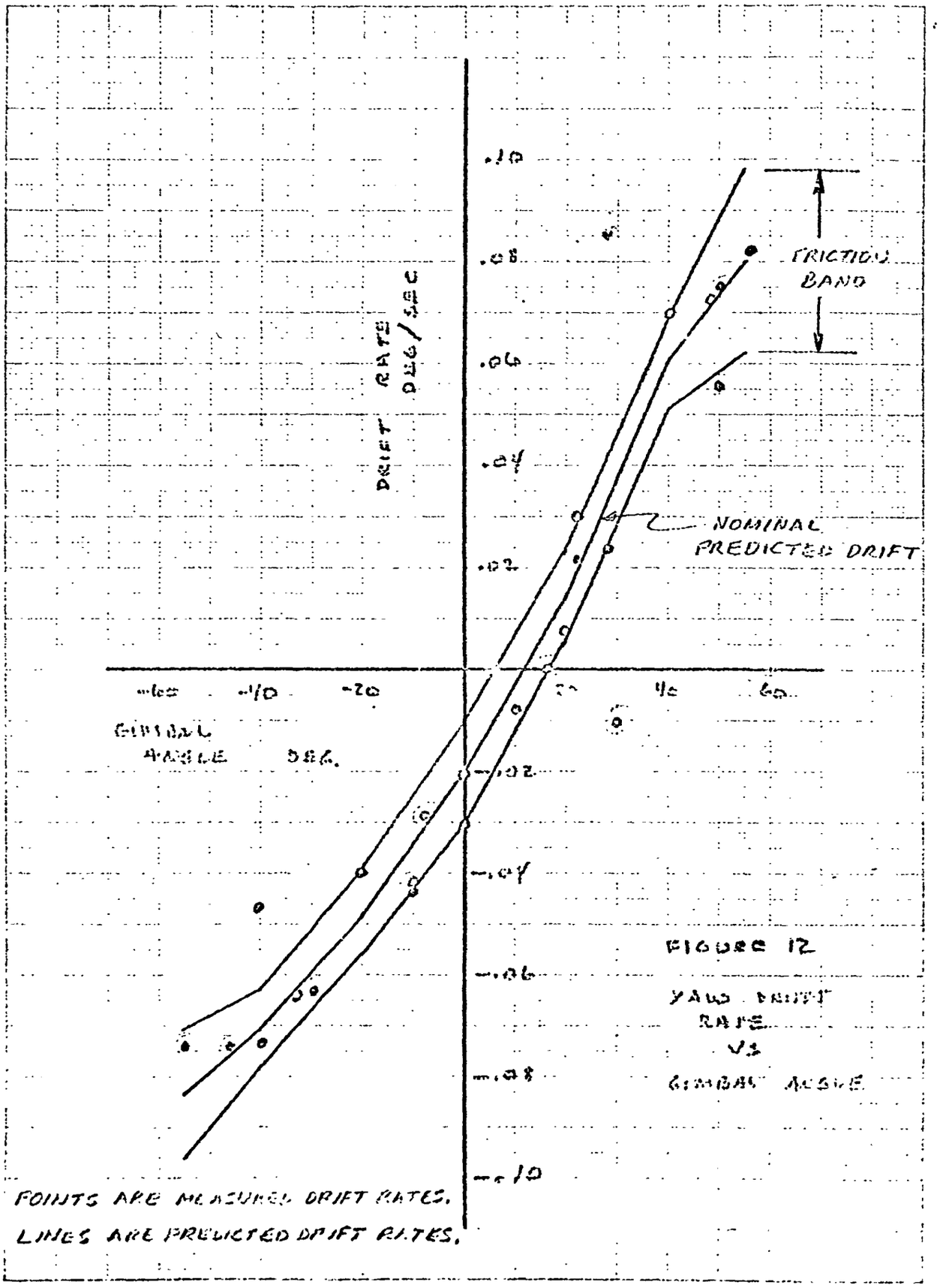

FIGURE 12

YAW DRIFT RATE VS GIMBAL ANGLE

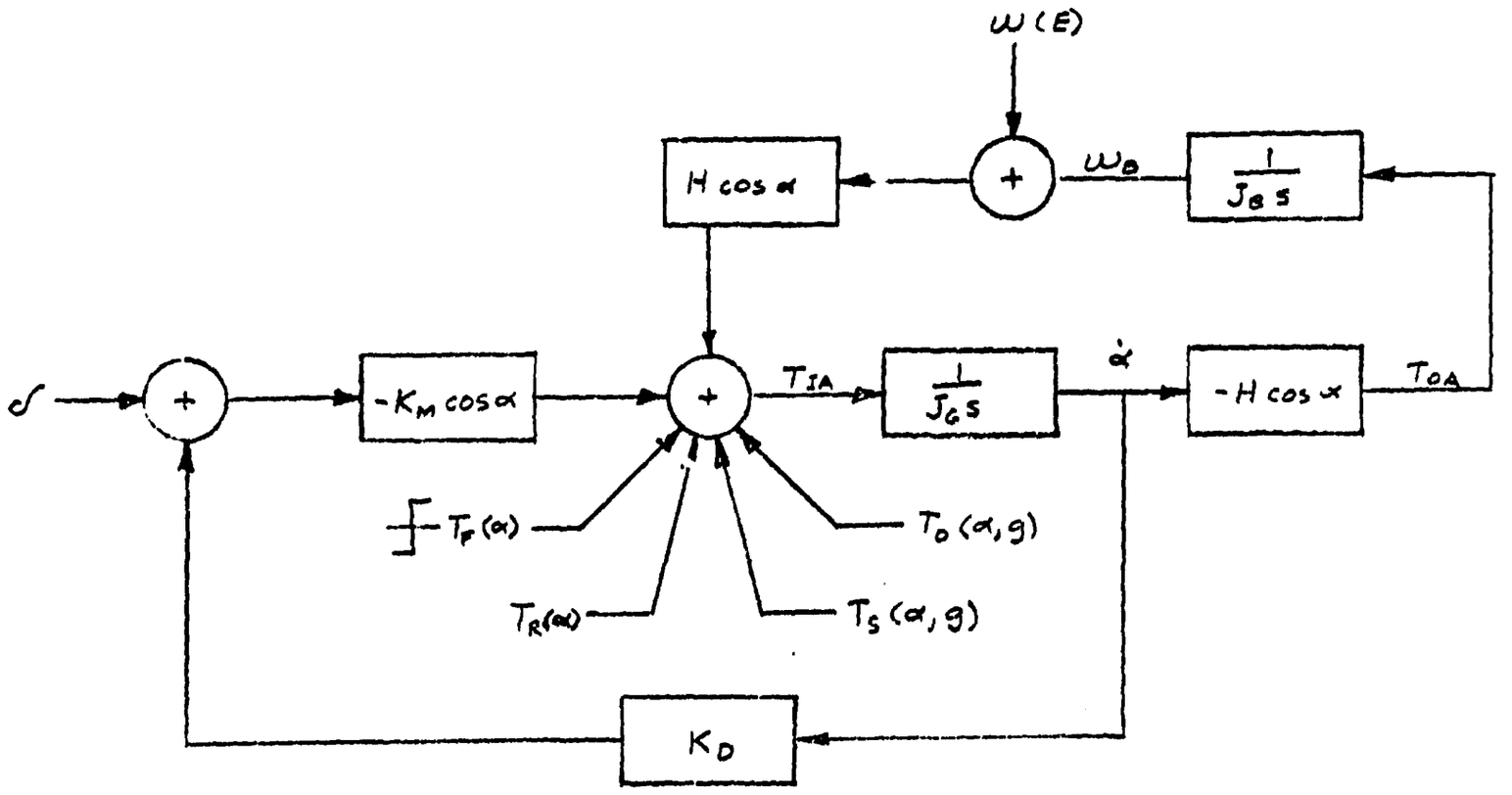

FIGURE 13 CMG ONE AXIS TORQUE DIAGRAM

α	Gimbal angle
J_G	Gimbal inertia
J_B	Body inertia
W_B	Body rate
W(E)	Earth rate component
H	Angular momentum of dual CMG, 2.1 ft-lb sec.

The equation expressing the sum of the torques at the gimbal is:

$$\sum T_{IA} = -\delta K_M \cos\alpha + T_R(\alpha) + W(E)\, H \cos\alpha$$

$$+ T_s(\alpha, g) + T_o(\alpha, g) + T_F(\alpha) + W_B\, H \cos\alpha$$

W (E) is the component of earth rate aligned with the output axis.

T_s is a function of gimbal angle and the g component directed perpendicular to the IA - SRA plane.

T_o is a function of gimbal angle and the g component directed perpendicular to the IA - OA plane.

T_R and T_F are functions of gimbal angle but are not sensitive to earth rate or gravity.

A series of fixed position tests were conducted to determine the values of the drift components for each of the CMG units in CMG Assembly. Prior to testing, a matrix of the combinations of drift components was constructed as shown in Table 1. Further symbol definitions are:

E = Earth rate = 7.25×10^{-5} rad/sec

β = Latitude at MMC - Denver = 39.5°

W (E) = E sin β or E cos β

Earth rate torques at zero gimbal angle are:

EH cos α cos β = .0226 in. oz.

= .00322 volts at command input.

EH cos α sin β = .0186 in. oz.

= .00264 volts at command input.

The matrix is related to the CMG axes as shown in Figure 14. T_s is positive when it causes a positive gimbal angle torque with an acceleration in the +OA direction. T_o is positive when it causes a positive gimbal angle torque with an acceleration in the +SRA direction.

FOR DRIFT COMPONENTS

ΣT_Y	ΣT_Z
	$T_R(\alpha) + EH\cos\alpha\cos\beta$
	$T_R(\alpha) - EH\cos\alpha\cos\beta$
$\cos\alpha\cos\beta$	$T_R(\alpha)$
$\cos\alpha\cos\beta$	$T_R(\alpha)$
	$T_R(\alpha) + EH\cos\alpha\cos\beta$
	$T_R(\alpha) - EH\cos\alpha\cos\beta$
$\cos\alpha\cos\beta$	$T_R(\alpha)$
$\cos\alpha\cos\beta$	$T_R(\alpha)$
$\cos\alpha\sin\beta - T_S\cos\alpha - T_O\sin\alpha$	$T_R(\alpha) + T_S\sin\alpha - T_O\cos\alpha$
$\cos\alpha\sin\beta - T_S\cos\alpha - T_O\sin\alpha$	$T_R(\alpha) + T_S\sin\alpha - T_O\cos\alpha$
$\cos\alpha\sin\beta - T_S\cos\alpha - T_O\sin\alpha$	$T_R(\alpha) + EH\cos\alpha\cos\beta + T_S\sin\alpha - T_O\cos\alpha$
$\cos\alpha\sin\beta - T_S\cos\alpha - T_O\sin\alpha$	$T_R(\alpha) - EH\cos\alpha\cos\beta + T_S\sin\alpha - T_O\cos\alpha$
$\cos\alpha\sin\beta + T_S\cos\alpha + T_O\sin\alpha$	$T_R(\alpha) - T_S\sin\alpha + T_O\cos\alpha$
$\cos\alpha\sin\beta + T_S\cos\alpha + T_O\sin\alpha$	$T_R(\alpha) - T_S\sin\alpha + T_O\cos\alpha$
$\cos\alpha\sin\beta + T_S\cos\alpha + T_O\sin\alpha$	$T_R(\alpha) + EH\cos\alpha\cos\beta - T_S\sin\alpha + T_O\cos\alpha$
$\cos\alpha\sin\beta + T_S\cos\alpha + T_O\sin\alpha$	$T_R(\alpha) - EH\cos\alpha\cos\beta - T_S\sin\alpha + T_O\cos\alpha$
$- T_S\sin\alpha + T_O\cos\alpha$	$T_R(\alpha) - EH\cos\alpha\sin\beta + T_S\cos\alpha + T_O\sin\alpha$
$- T_S\sin\alpha + T_O\cos\alpha$	$T_R(\alpha) - EH\cos\alpha\sin\beta + T_S\cos\alpha + T_O\sin\alpha$
$\cos\alpha\cos\beta - T_S\sin\alpha + T_O\cos\alpha$	$T_R(\alpha) - EH\cos\alpha\sin\beta + T_S\cos\alpha + T_O\sin\alpha$
$\cos\alpha\cos\beta - T_S\sin\alpha + T_O\cos\alpha$	$T_R(\alpha) - EH\cos\alpha\sin\beta + T_S\cos\alpha + T_O\sin\alpha$
$+ T_S\sin\alpha - T_O\cos\alpha$	$T_R(\alpha) + EH\cos\alpha\sin\beta - T_S\cos\alpha - T_O\sin\alpha$
$+ T_S\sin\alpha - T_O\cos\alpha$	$T_R(\alpha) + EH\cos\alpha\sin\beta - T_S\cos\alpha - T_O\sin\alpha$
$\cos\alpha\cos\beta + T_S\sin\alpha - T_O\cos\alpha$	$T_R(\alpha) + EH\cos\alpha\sin\beta - T_S\cos\alpha - T_O\sin\alpha$
$\cos\alpha\cos\beta + T_S\sin\alpha - T_O\cos\alpha$	$T_R(\alpha) + EH\cos\alpha\sin\beta - T_S\cos\alpha - T_O\sin\alpha$

TABLE 1. POSITION MATRIX FOR DRIFT COMPONENTS

ΣT_X	ΣT_Y	
$\cos\beta + T_S \cos\alpha + T_O \sin\alpha$	$T_R(\alpha)$	$T_R(\alpha)$
$\alpha\cos\beta + T_S \cos\alpha + T_O \sin\alpha$	$T_R(\alpha)$	$T_R(\alpha)$
$\alpha\cos\beta + T_S \cos\alpha + T_O \sin\alpha$	$T_R(\alpha) + EH\cos\alpha\cos\beta$	$T_R(\alpha)$
$\alpha\cos\beta + T_S \cos\alpha + T_O \sin\alpha$	$T_R(\alpha) - EH\cos\alpha\cos\beta$	$T_R(\alpha)$
$\alpha\cos\beta - T_S \cos\alpha - T_O \sin\alpha$	$T_R(\alpha)$	$T_R(\alpha)$
$\alpha\cos\beta - T_S \cos\alpha - T_O \sin\alpha$	$T_R(\alpha)$	$T_R(\alpha)$
$\alpha\cos\beta - T_S \cos\alpha - T_O \sin\alpha$	$T_R(\alpha) - EH\cos\alpha\cos\beta$	$T_R(\alpha)$
$\alpha\cos\beta - T_S \cos\alpha - T_O \sin\alpha$	$T_R(\alpha) + EH\cos\alpha\cos\beta$	$T_R(\alpha)$
$\alpha\cos\beta - T_S \sin\alpha + T_O \cos\alpha$	$T_R(\alpha) + EH\cos\alpha\sin\beta - T_S\cos\alpha - T_O\sin\alpha$	$T_R(\alpha)$
$\alpha\cos\beta - T_S \sin\alpha + T_O \cos\alpha$	$T_R(\alpha) + EH\cos\alpha\sin\beta - T_S\cos\alpha - T_O\sin\alpha$	$T_R(\alpha)$
$- T_S \sin\alpha + T_O \cos\alpha$	$T_R(\alpha) + EH\cos\alpha\sin\beta - T_S\cos\alpha - T_O\sin\alpha$	$T_R(\alpha)$
$- T_S \sin\alpha + T_O \cos\alpha$	$T_R(\alpha) + EH\cos\alpha\sin\beta - T_S\cos\alpha - T_O\sin\alpha$	$T_R(\alpha)$
$\alpha\cos\beta + T_S \sin\alpha - T_O \cos\alpha$	$T_R(\alpha) - EH\cos\alpha\sin\beta + T_S\cos\alpha + T_O\sin\alpha$	$T_R(\alpha)$
$\alpha\cos\beta + T_S \sin\alpha - T_O \cos\alpha$	$T_R(\alpha) - EH\cos\alpha\sin\beta + T_S\cos\alpha + T_O\sin\alpha$	$T_R(\alpha)$
$+ T_S \sin\alpha - T_O \cos\alpha$	$T_R(\alpha) - EH\cos\alpha\sin\beta + T_S\cos\alpha + T_O\sin\alpha$	$T_R(\alpha)$
$+ T_S \sin\alpha - T_O \cos\alpha$	$T_R(\alpha) - EH\cos\alpha\sin\beta + T_S\cos\alpha + T_O\sin\alpha$	$T_R(\alpha)$
$\alpha\cos\beta$	$T_R(\alpha) - T_S\sin\alpha + T_O\cos\alpha$	$T_R(\alpha)$
$\alpha\cos\beta$	$T_R(\alpha) - T_S\sin\alpha + T_O\cos\alpha$	$T_R(\alpha)$
	$T_R(\alpha) - EH\cos\alpha\cos\beta - T_S\sin\alpha + T_O\cos\alpha$	$T_R(\alpha)$
	$T_R(\alpha) + EH\cos\alpha\cos\beta - T_S\sin\alpha + T_O\cos\alpha$	$T_R(\alpha)$
$\alpha\cos\beta$	$T_R(\alpha) + T_S\sin\alpha - T_O\cos\alpha$	$T_R(\alpha)$
$\alpha\cos\beta$	$T_R(\alpha) + T_S\sin\alpha - T_O\cos\alpha$	$T_R(\alpha)$
	$T_R(\alpha) + EH\cos\alpha\cos\beta + T_S\sin\alpha - T_O\cos\alpha$	$T_R(\alpha)$
	$T_R(\alpha) - EH\cos\alpha\cos\beta + T_S\sin\alpha - T_O\cos\alpha$	$T_R(\alpha)$

TABLE 1. POSITION MATI

POSITION	ΣT_x	
X DOWN, Z NORTH	$T_R(\alpha) - EH\cos\alpha\cos\beta + T_S\cos\alpha + T_O\sin\alpha$	$T_R(\alpha)$
" Z SOUTH	$T_R(\alpha) - EH\cos\alpha\cos\beta + T_S\cos\alpha + T_O\sin\alpha$	$T_R(\alpha)$
" Z EAST	$T_R(\alpha) - EH\cos\alpha\cos\beta + T_S\cos\alpha + T_O\sin\alpha$	$T_R(\alpha) + E$
" Z WEST	$T_R(\alpha) - EH\cos\alpha\cos\beta + T_S\cos\alpha + T_O\sin\alpha$	$T_R(\alpha) - E$
X UP, Z NORTH	$T_R(\alpha) + EH\cos\alpha\cos\beta - T_S\cos\alpha - T_O\sin\alpha$	$T_R(\alpha)$
" Z SOUTH	$T_R(\alpha) + EH\cos\alpha\cos\beta - T_S\cos\alpha - T_O\sin\alpha$	$T_R(\alpha)$
" Z EAST	$T_R(\alpha) + EH\cos\alpha\cos\beta - T_S\cos\alpha - T_O\sin\alpha$	$T_R(\alpha) - E$
" Z WEST	$T_R(\alpha) + EH\cos\alpha\cos\beta - T_S\cos\alpha - T_O\sin\alpha$	$T_R(\alpha) + E$
Y DOWN, X NORTH	$T_R(\alpha) + EH\cos\alpha\cos\beta - T_S\sin\alpha + T_O\cos\alpha$	$T_R(\alpha) + E$
" X SOUTH	$T_R(\alpha) - EH\cos\alpha\cos\beta - T_S\sin\alpha + T_O\cos\alpha$	$T_R(\alpha) + E$
" X EAST	$T_R(\alpha) - T_S\sin\alpha + T_O\cos\alpha$	$T_R(\alpha) +$
" X WEST	$T_R(\alpha) - T_S\sin\alpha + T_O\cos\alpha$	$T_R(\alpha) + E$
Y UP, X NORTH	$T_R(\alpha) + EH\cos\alpha\cos\beta + T_S\sin\alpha - T_O\cos\alpha$	$T_R(\alpha) - E$
" X SOUTH	$T_R(\alpha) - EH\cos\alpha\cos\beta + T_S\sin\alpha - T_O\cos\alpha$	$T_R(\alpha) - E$
" X EAST	$T_R(\alpha) + T_S\sin\alpha - T_O\cos\alpha$	$T_R(\alpha) - E$
" X WEST	$T_R(\alpha) + T_S\sin\alpha - T_O\cos\alpha$	$T_R(\alpha) - E$
Z DOWN, X NORTH	$T_R(\alpha) + EH\cos\alpha\cos\beta$	$T_R(\alpha)$
" X SOUTH	$T_R(\alpha) - EH\cos\alpha\cos\beta$	$T_R(\alpha)$
" X EAST	$T_R(\alpha)$	$T_R(\alpha) -$
" X WEST	$T_R(\alpha)$	$T_R(\alpha) +$
Z UP, X NORTH	$T_R(\alpha) + EH\cos\alpha\cos\beta$	$T_R(\alpha)$
X SOUTH	$T_R(\alpha) - EH\cos\alpha\cos\beta$	$T_R(\alpha)$
X EAST	$T_R(\alpha)$	$T_R(\alpha) +$
X WEST	$T_R(\alpha)$	$T_R(\alpha) - E$

TABLE 1. POS

POSITION	ΣT_x
X DOWN, Z NORTH	$T_R(\alpha) - EH\cos\alpha\cos\beta + T_S\cos\alpha + T_O\sin\alpha$
" Z SOUTH	$T_R(\alpha) - EH\cos\alpha\cos\beta + T_S\cos\alpha + T_O\sin\alpha$
" Z EAST	$T_R(\alpha) - EH\cos\alpha\cos\beta + T_S\cos\alpha + T_O\sin\alpha$
" Z WEST	$T_R(\alpha) - EH\cos\alpha\cos\beta + T_S\cos\alpha + T_O\sin\alpha$
X UP, Z NORTH	$T_R(\alpha) + EH\cos\alpha\cos\beta - T_S\cos\alpha - T_O\sin\alpha$
" Z SOUTH	$T_R(\alpha) + EH\cos\alpha\cos\beta - T_S\cos\alpha - T_O\sin\alpha$
" Z EAST	$T_R(\alpha) + EH\cos\alpha\cos\beta - T_S\cos\alpha - T_O\sin\alpha$
" Z WEST	$T_R(\alpha) + EH\cos\alpha\cos\beta - T_S\cos\alpha - T_O\sin\alpha$
Y DOWN, X NORTH	$T_R(\alpha) + EH\cos\alpha\cos\beta - T_S\sin\alpha + T_O\cos\alpha$
" X SOUTH	$T_R(\alpha) - EH\cos\alpha\cos\beta - T_S\sin\alpha + T_O\cos\alpha$
" X EAST	$T_R(\alpha) - T_S\sin\alpha + T_O\cos\alpha$
" X WEST	$T_R(\alpha) - T_S\sin\alpha + T_O\cos\alpha$
Y UP, X NORTH	$T_R(\alpha) + EH\cos\alpha\cos\beta + T_S\sin\alpha - T_O\cos\alpha$
" X SOUTH	$T_R(\alpha) - EH\cos\alpha\cos\beta + T_S\sin\alpha - T_O\cos\alpha$
" X EAST	$T_R(\alpha) + T_S\sin\alpha - T_O\cos\alpha$
" X WEST	$T_R(\alpha) + T_S\sin\alpha - T_O\cos\alpha$
Z DOWN, X NORTH	$T_R(\alpha) + EH\cos\alpha\cos\beta$
" X SOUTH	$T_R(\alpha) - EH\cos\alpha\cos\beta$
" X EAST	$T_R(\alpha)$
" X WEST	$T_R(\alpha)$
Z UP, X NORTH	$T_R(\alpha) + EH\cos\alpha\cos\beta$
X SOUTH	$T_R(\alpha) - EH\cos\alpha\cos\beta$
X EAST	$T_R(\alpha)$
X WEST	$T_R(\alpha)$

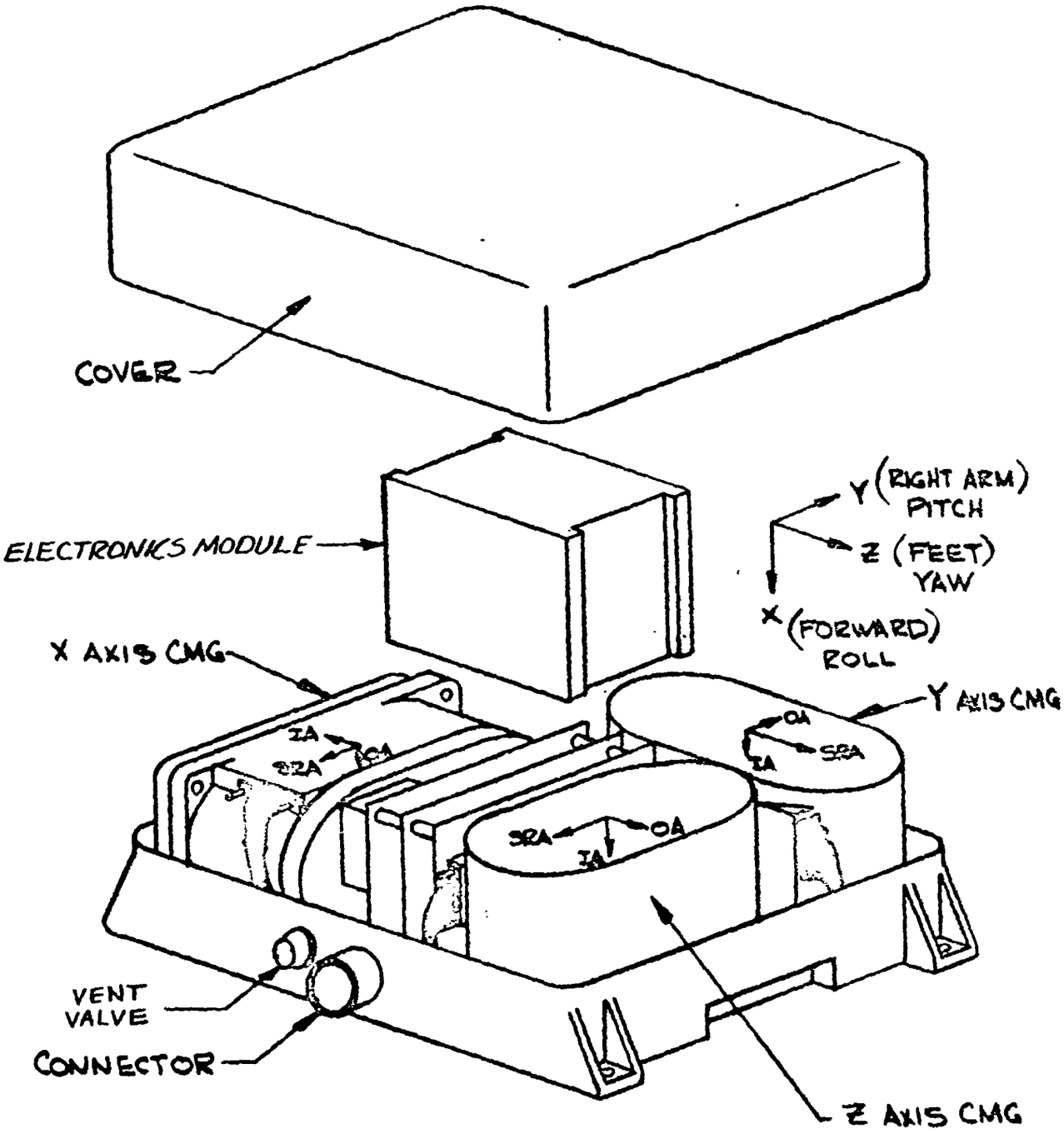

FIGURE 14 CMG COORDINATE SYSTEM

Initially, the CMGA was mounted Z down and X east so that only the reaction and friction torque components were present. The friction torque component was determined by slewing the gimbal in one direction and then bringing the gimbal angle to zero by small changes in command input. The process was repeated but with the gimbal slewed in the opposite direction. The friction torque was half the difference between the two command inputs multiplied by K_M (7.04 in. oz/volt).

Further experimentation resulted in an improved technique that was used throughout the remainder of the test. The gimbal was brought to zero by input commands and then the command was slowly changed to determine the input necessary to break away from zero angle in the positive and negative directions. Again the friction torque was obtained by taking half the difference between these two voltage readings. The value for T_R was then proportional to the average of the two readings (or half the sum).

The CMGA was then placed Z down, X south and the average for the two zero angle breakaway voltages was determined. From the table, it is seen that this value was the input voltage equivalent of:

$$\sum T_x = T_R(\alpha) - EH \cos\alpha \cos\beta$$

This reading subtracted from the Z down X east reading should yield the earth rate component. The result was .0045 volts compared to the previously determined value of .0032 volts and the sign was correct. This result, the fact that a component of earth rate could be grossly determined, gave high confidence to the test technique and the test was continued.

The following readings were made at the indicated CMG positions:

Y down, X west	$\sum T_x$	$\alpha = 0^\circ$
	$\sum T_y$	$\alpha = 0^\circ$
	$\sum T_z$	$\alpha = 0^\circ$
Z down, X east	$\sum T_x$ and T_F	$\alpha = 0^\circ, \pm 20^\circ, \pm 40^\circ, \pm 55^\circ$
	$\sum T_y$	$\alpha = 0^\circ$
	$\sum T_z$	$\alpha = 0^\circ$
X down, Z north	$\sum T_x$	$\alpha = 0^\circ$
	$\sum T_y$ and T_F	$\alpha = 0^\circ, \pm 20^\circ, \pm 40^\circ, \pm 55^\circ$
	$\sum T_y$	$\alpha = 0^\circ$
X down, Z east	$\sum T_x$	$\alpha = 0^\circ$
	$\sum T_y$	$\alpha = 0^\circ$
	$\sum T_z$ and T_F	$\alpha = 0^\circ, \pm 20^\circ, \pm 40^\circ, \pm 55^\circ$

The values of all the drift components were determined by combining these readings. Table 2 lists the mass unbalance torques. Note that all mass unbalance torques are below 0.08 in. oz. These torques are not present in zero g.

The friction torques are shown in Figures 15, 16 and 17 compared with previous Sperry data. The Sperry data is a composite of all data during DD testing. Note that the friction has generally increased but that the gimbal bearings have not appreciably degraded during the life test. The friction increase at the high gimbal angles is not surprising in view of the many impacts into the stops during the life test.

The gimbal reaction torques are plotted in Figures 18, 19, and 20. The Sperry data was from the final functional test prior to ship to MMC. The X gyro data from Sperry includes the mass unbalance torques for the X down position so these torques have been combined in the MMC data to allow a direct comparison. Note that the Y and Z data shows essentially no change while the X gyro shifted about 0.25 in. oz.

As previously stated the gimbal disturbance torques cause inertial drift of the body. The MMC generated disturbance torque values were combined and converted to predicted drift levels to compare with the air bearing drift test. The position equation for X down was used for the X gyro, Y down for the Y gyro, and Z down for the Z gyro. The nominal predicted drift rate and a band that includes the friction torque range are shown in Figures 10, 11, and 12 along with the actual measured rates on the air bearing table. These figures are important for two reasons. First, they show that inertial drift can be accurately predicted after determining the disturbance torque components with fixed position tests. Second, they show that the CMG's are better than 0.1 deg/sec quality even after extensive and quite severe life testing.

The largest disturbance torque is the reaction torque which is caused primarily by the interaction of the residual torque of the two torquer motors. Sperry expects this effect to be greatly reduced in the flight article CMG's because of improved Aeroflex motors. The reaction torque shift in the X gyro is interesting but may have been caused by a bias in the Sperry data. The general conclusion is that the Sperry CMG is a rugged, quality actuator and sensor when operated within its gimbal rate limits.

TABLE 2

MASS UNBALANCE TORQUES

	X CMG	Y CMG	Z CMG
T_o (volts at $\alpha = 0$)	+.008	+.0019	+.0069
(in oz)	+.056	+.013	+.049
T_s (volts at $\alpha = 0$)	+.0114	-.0017	+.0057
(in oz)	+.080	-.012	+.040

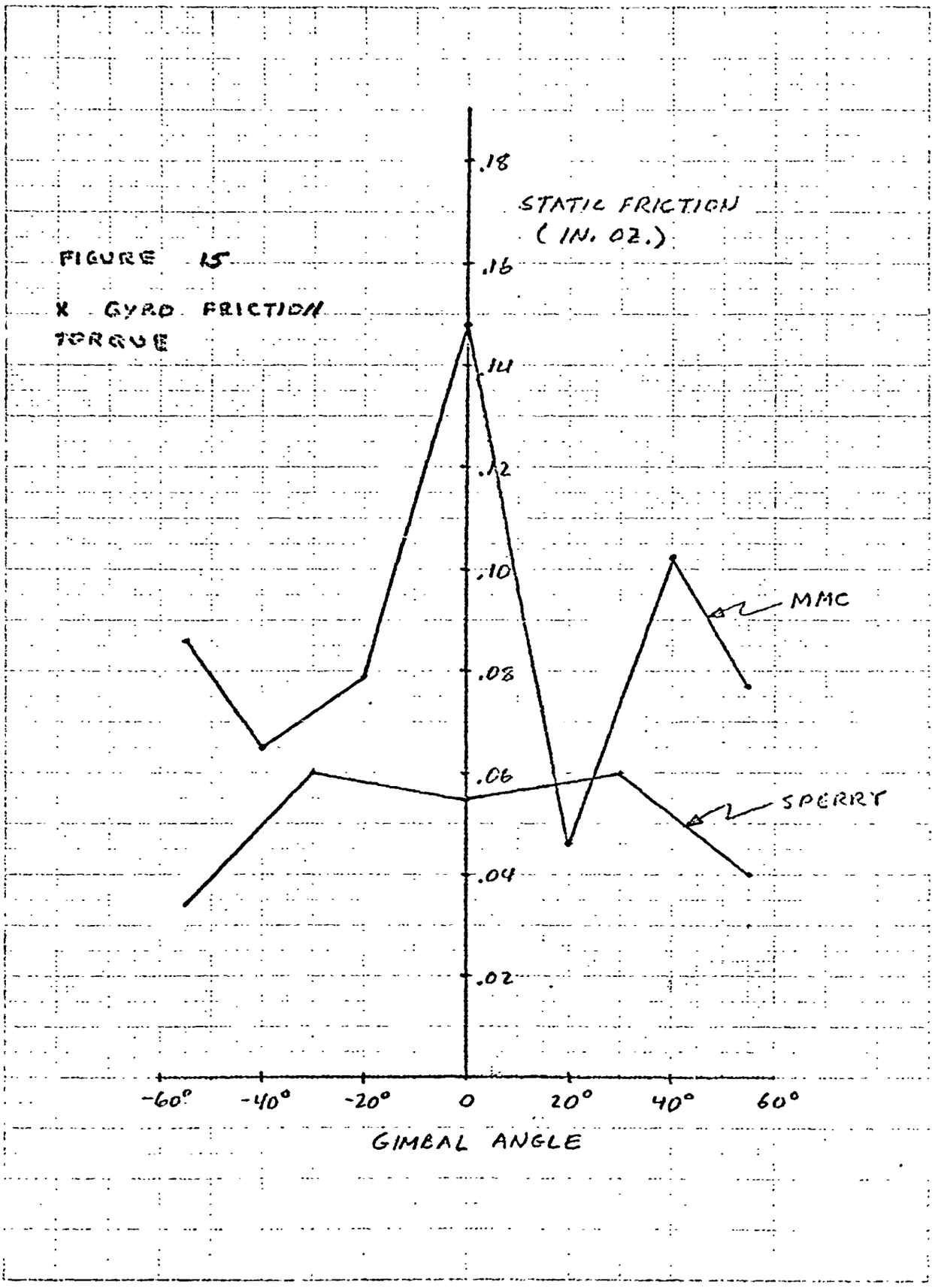

FIGURE 15

X GYRO FRICTION TORQUE

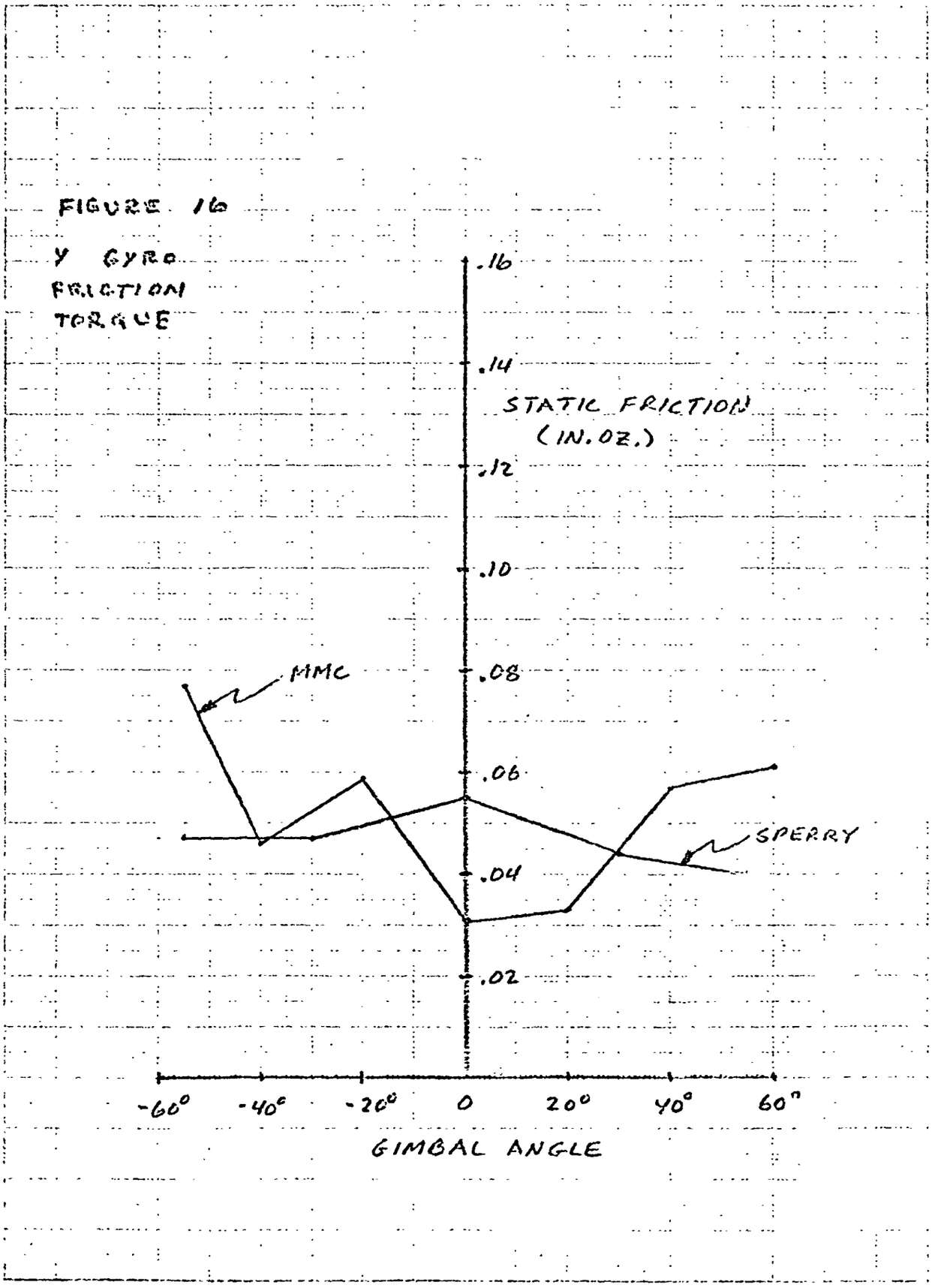
FIGURE 16
Y GYRO
FRICTION
TORQUE
.16
.14
STATIC FRICTION
(IN. OZ.)
.12
.10
.08
.06
.04
.02
MMC
SPERRY
-60°
-40°
-20°
0
20°
40°
60°
GIMBAL ANGLE

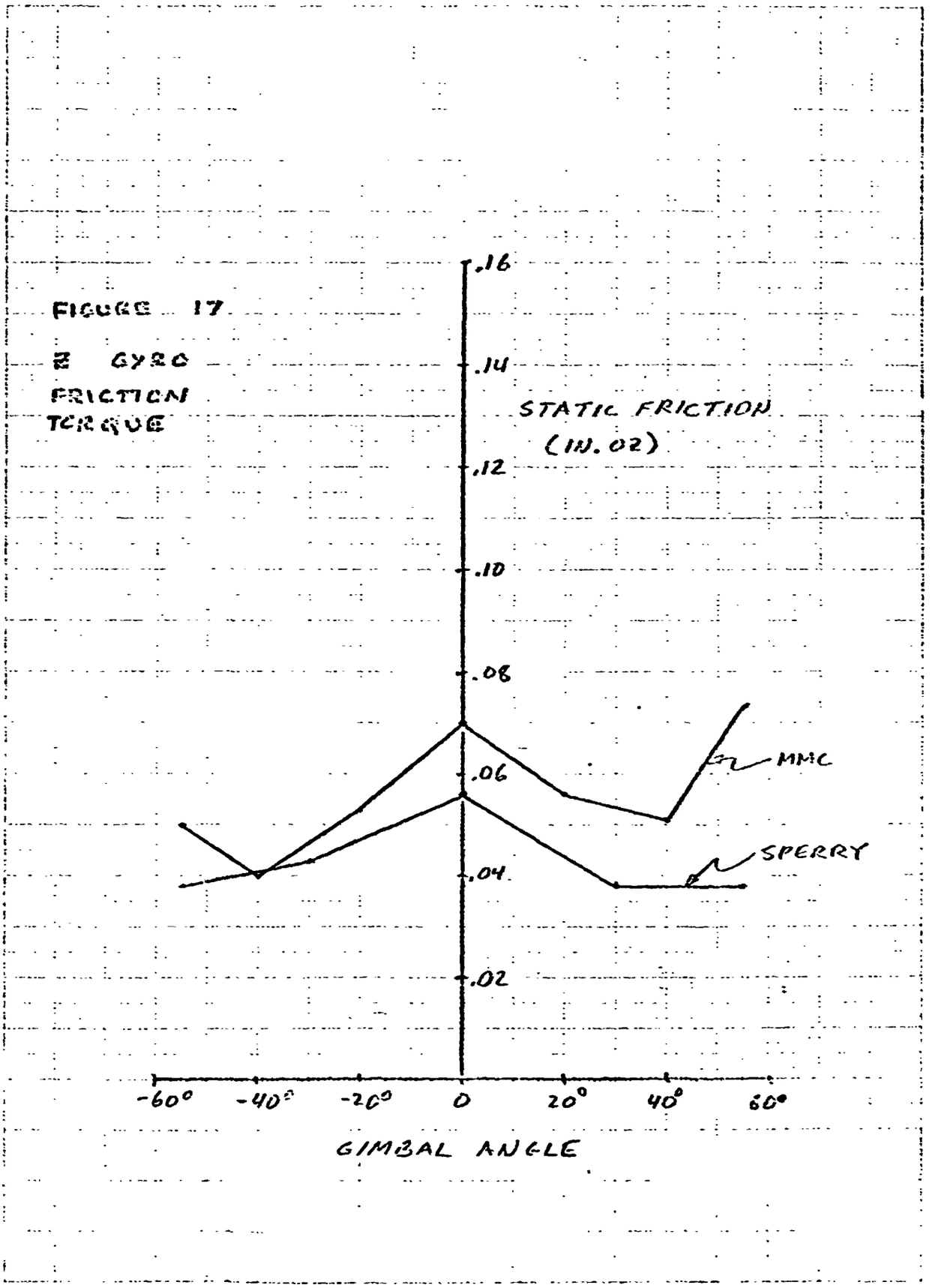
FIGURE 17
Z GYRO
FRICTION
TORQUE
STATIC FRICTION
(IN. OZ)
.16
.14
.12
.10
.08
.06
.04
.02
MMC
SPERRY
-60°
-40°
-20°
0
20°
40°
60°
GIMBAL ANGLE

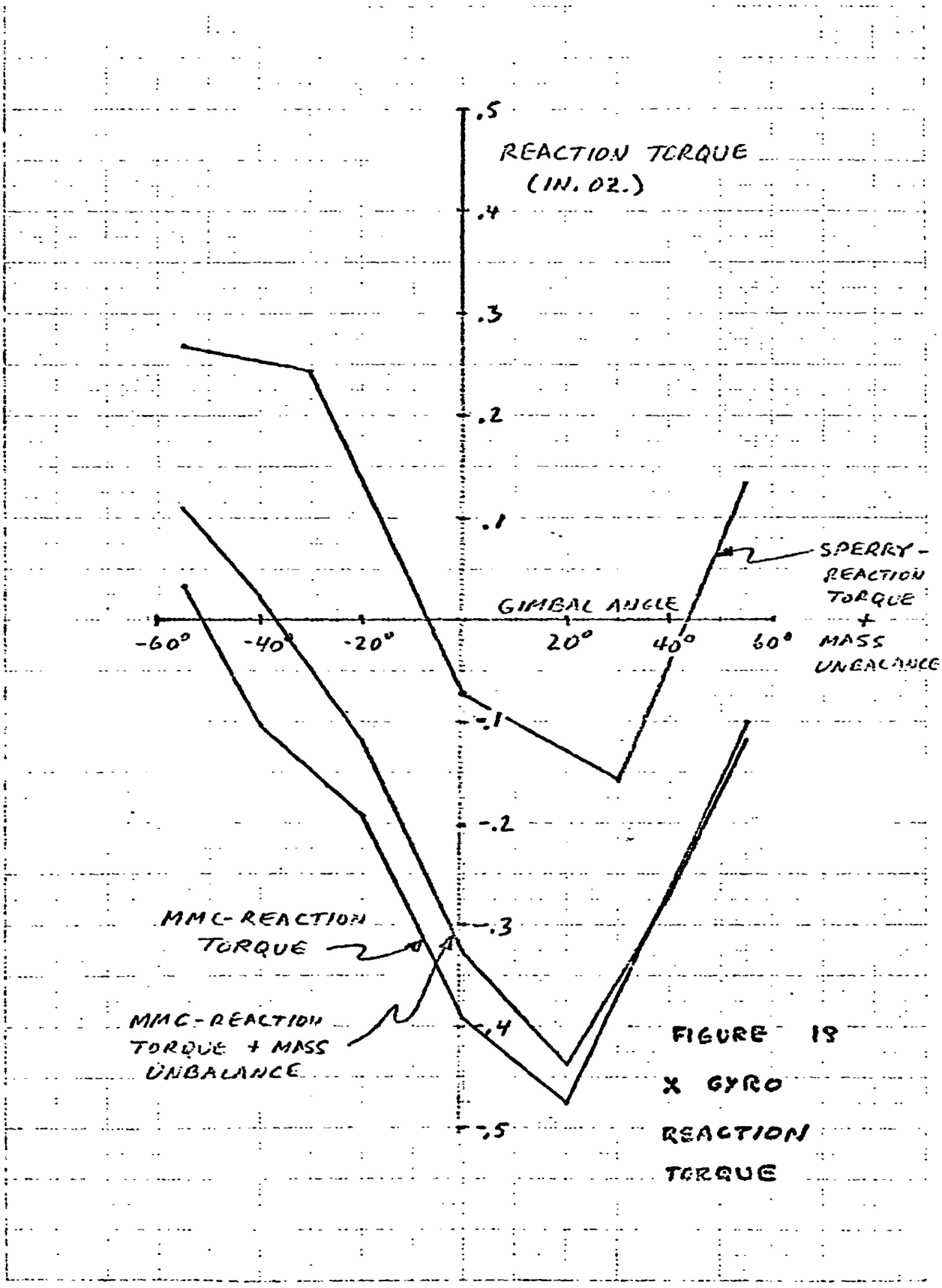

FIGURE 18
X GYRO
REACTION
TORQUE

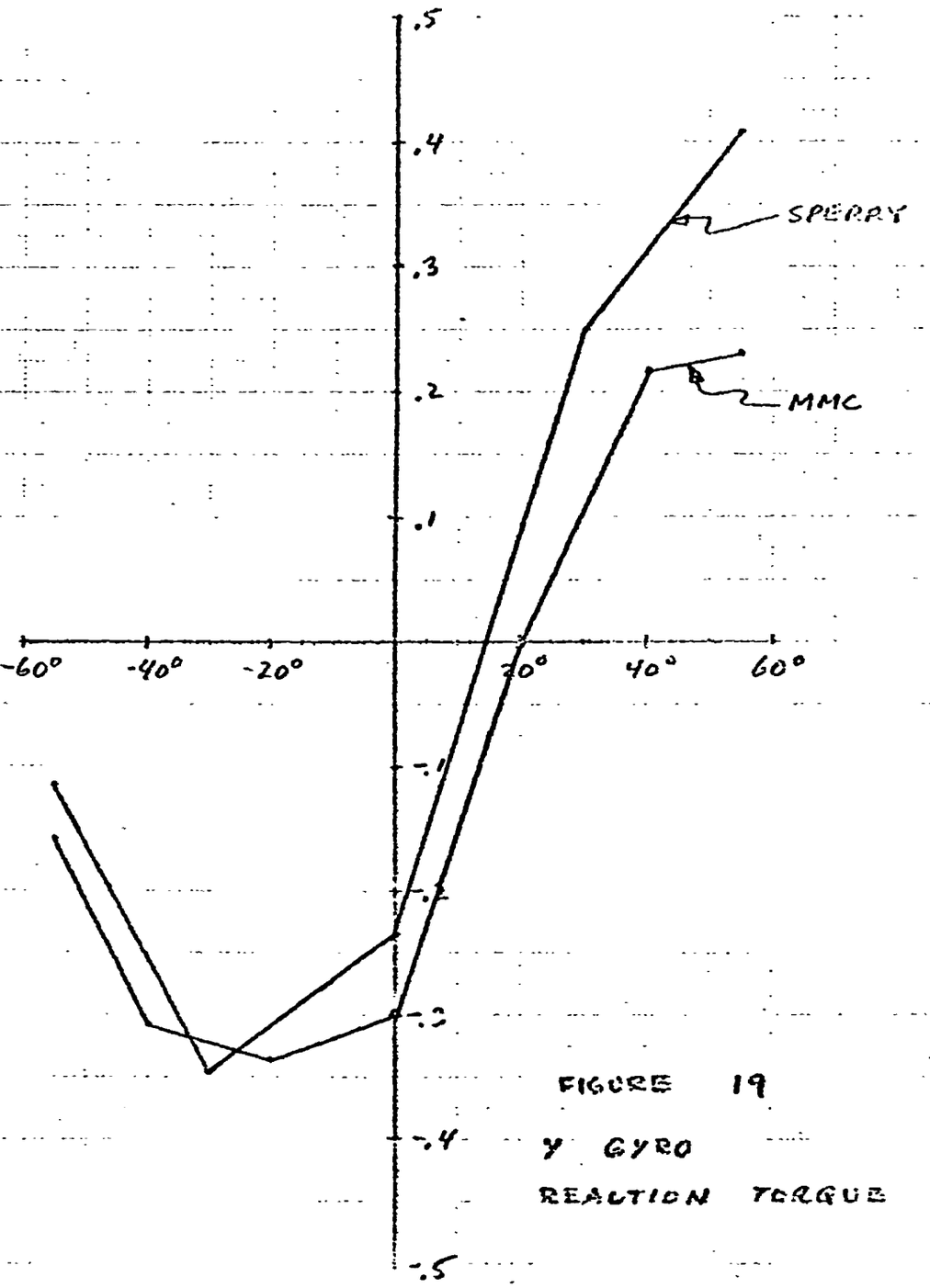

FIGURE 19

Y GYRO

REACTION TORQUE

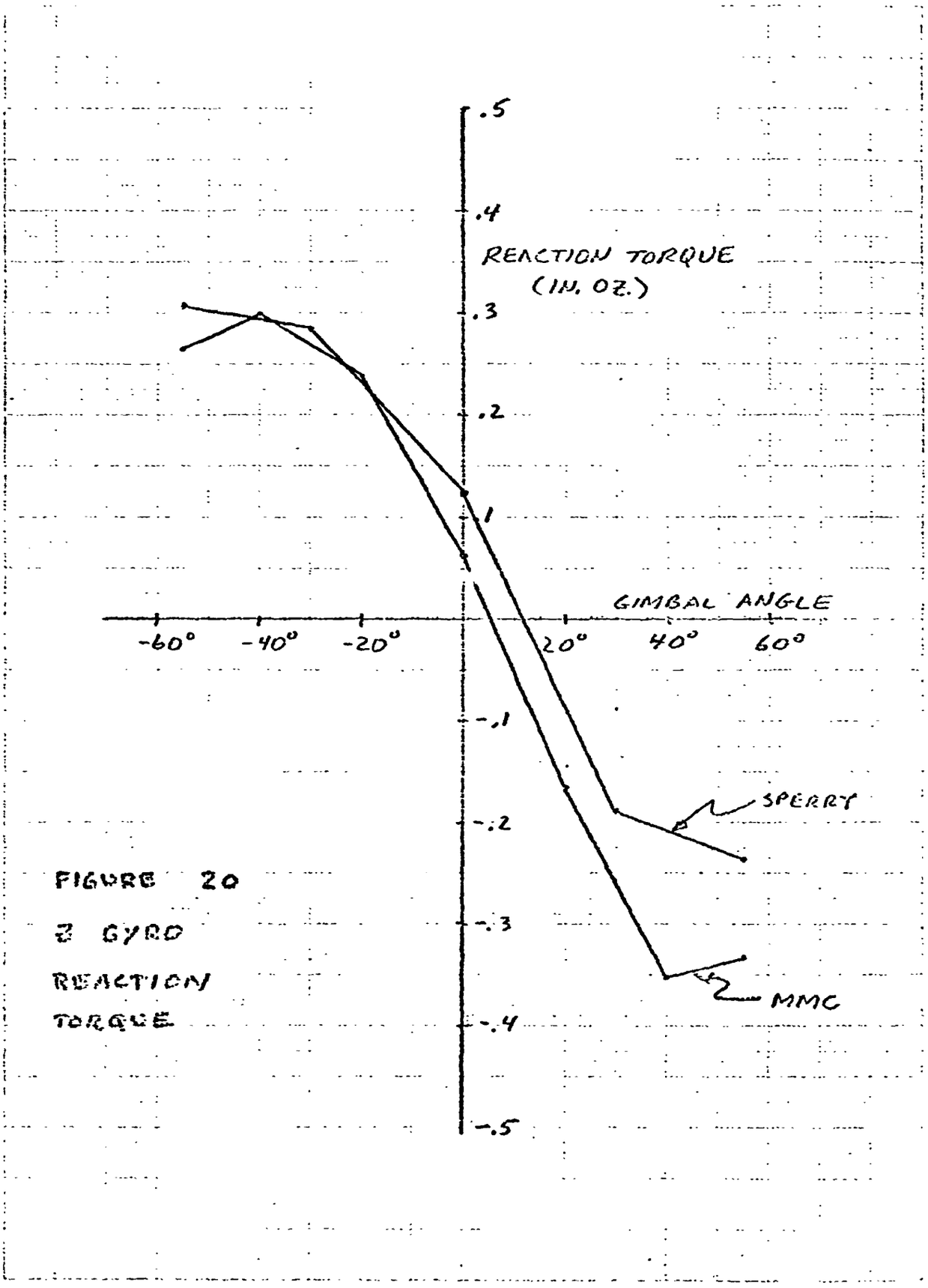

FIGURE 20

Z GYRO

REACTION

TORQUE